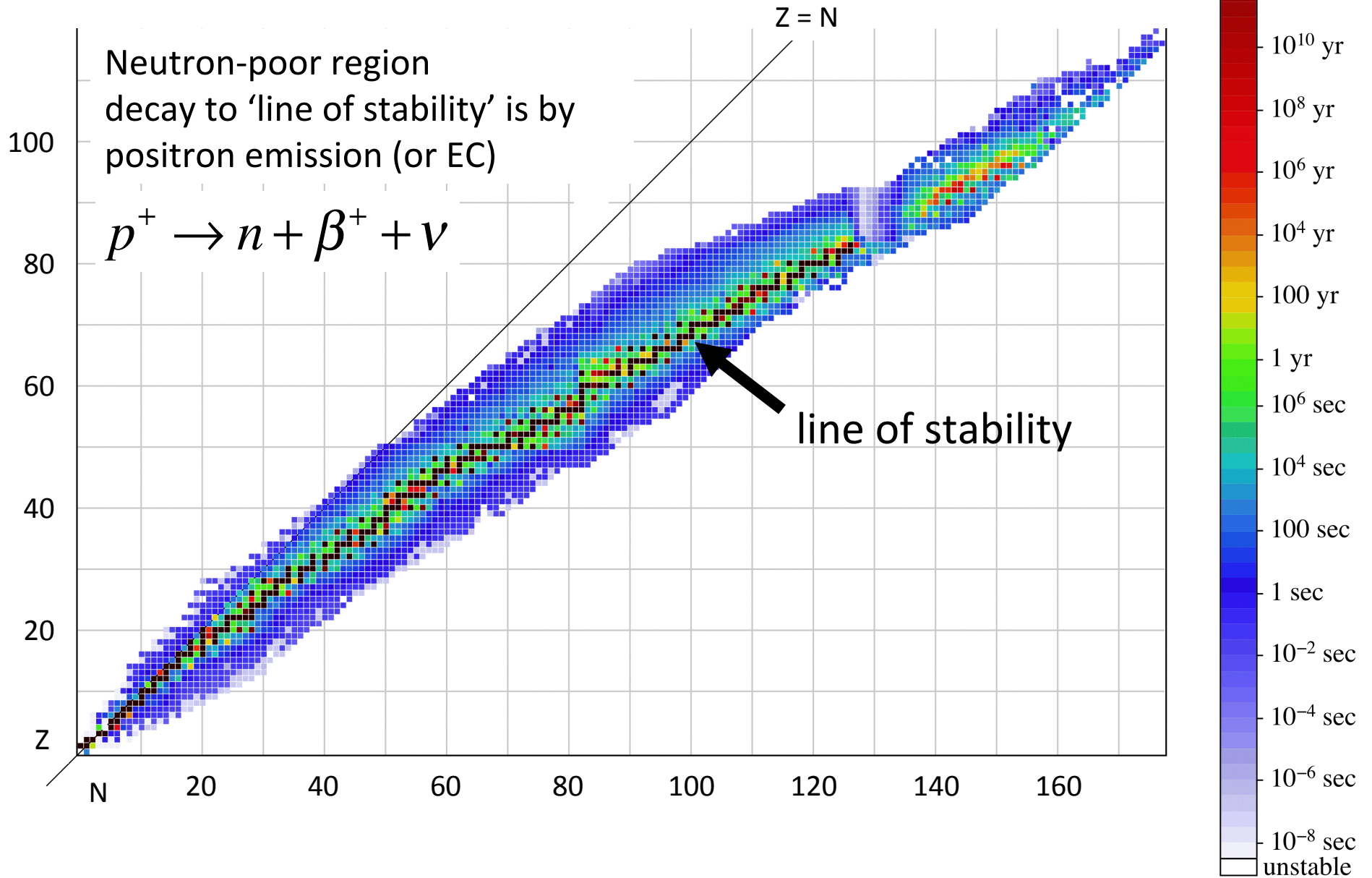
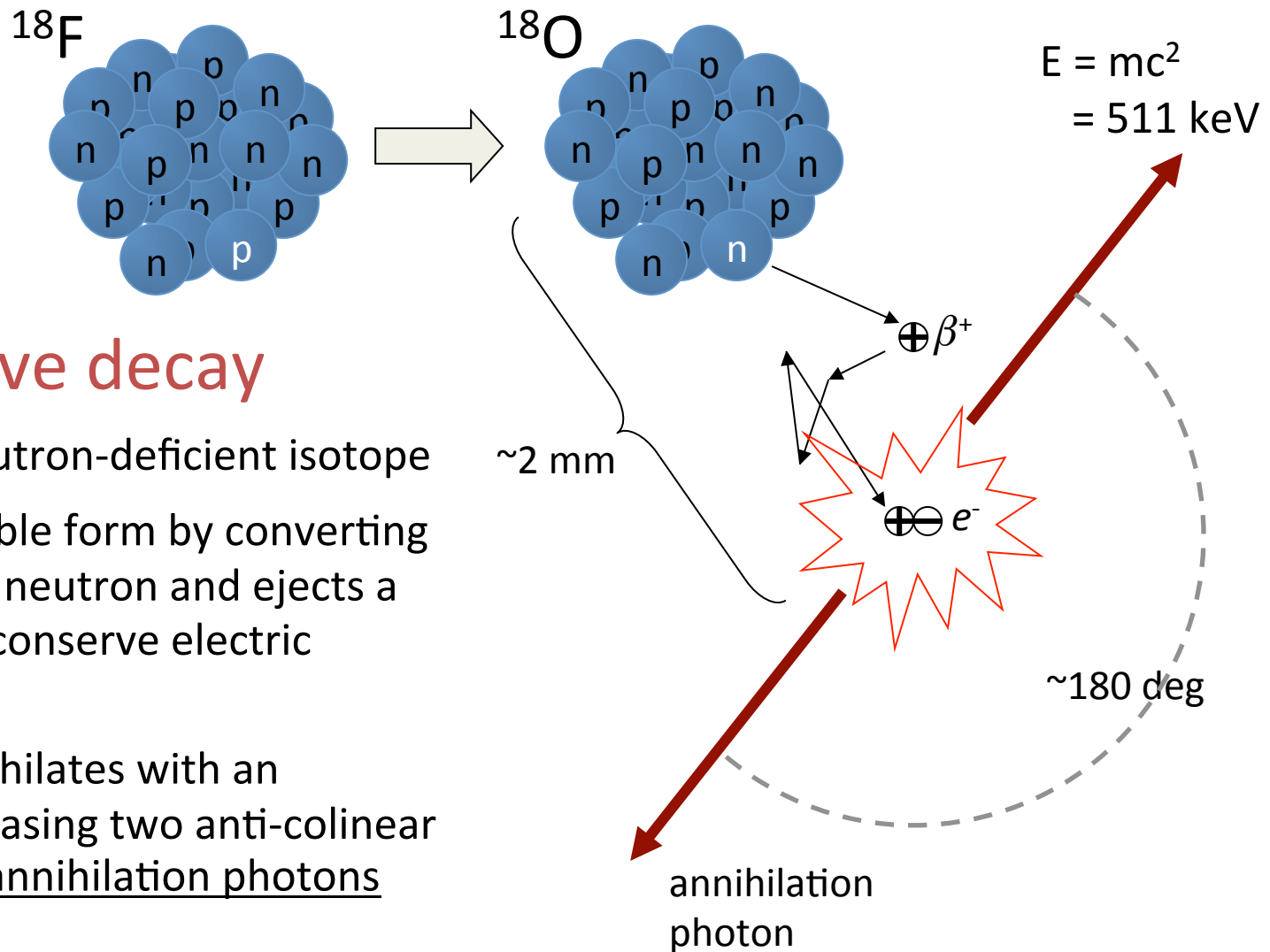


Positron Emission Tomography (PET) and PET/CT

Positron (β^+) Emission



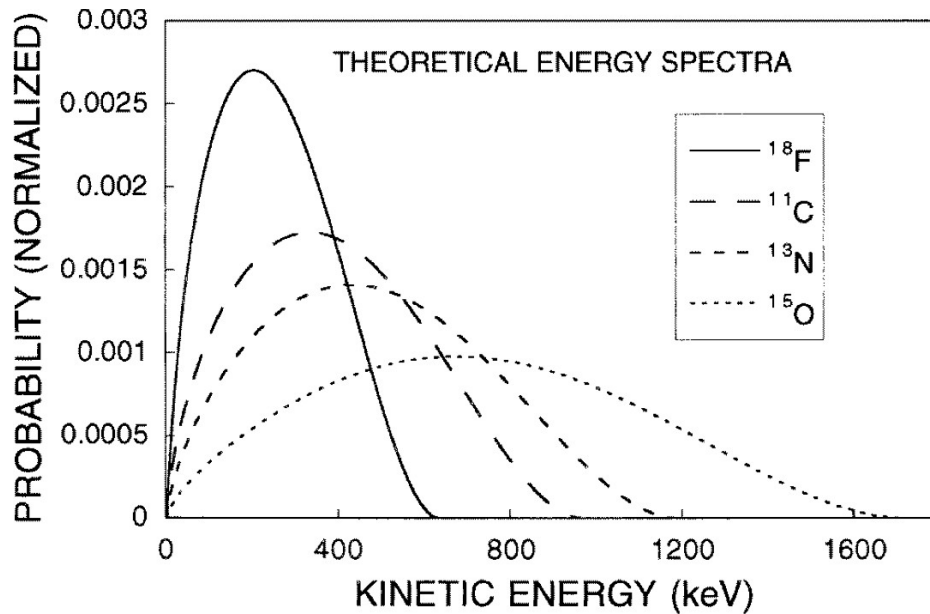
Positron Emission



Radioactive decay

- start with neutron-deficient isotope
- decays to stable form by converting a proton to a neutron and ejects a 'positron' to conserve electric charge
- positron annihilates with an electron, releasing two anti-colinear high-energy annihilation photons

Energy Spectrum of Emitted Positrons



Levin PMB 1999

Isotope	Max β^+ (Mev)
^{11}C	0.97
^{13}N	1.20
^{15}O	1.74
^{18}F	0.64
^{64}Cu	0.66
^{68}Ga	1.90
^{82}Rb	3.35
^{94}Tc	2.47

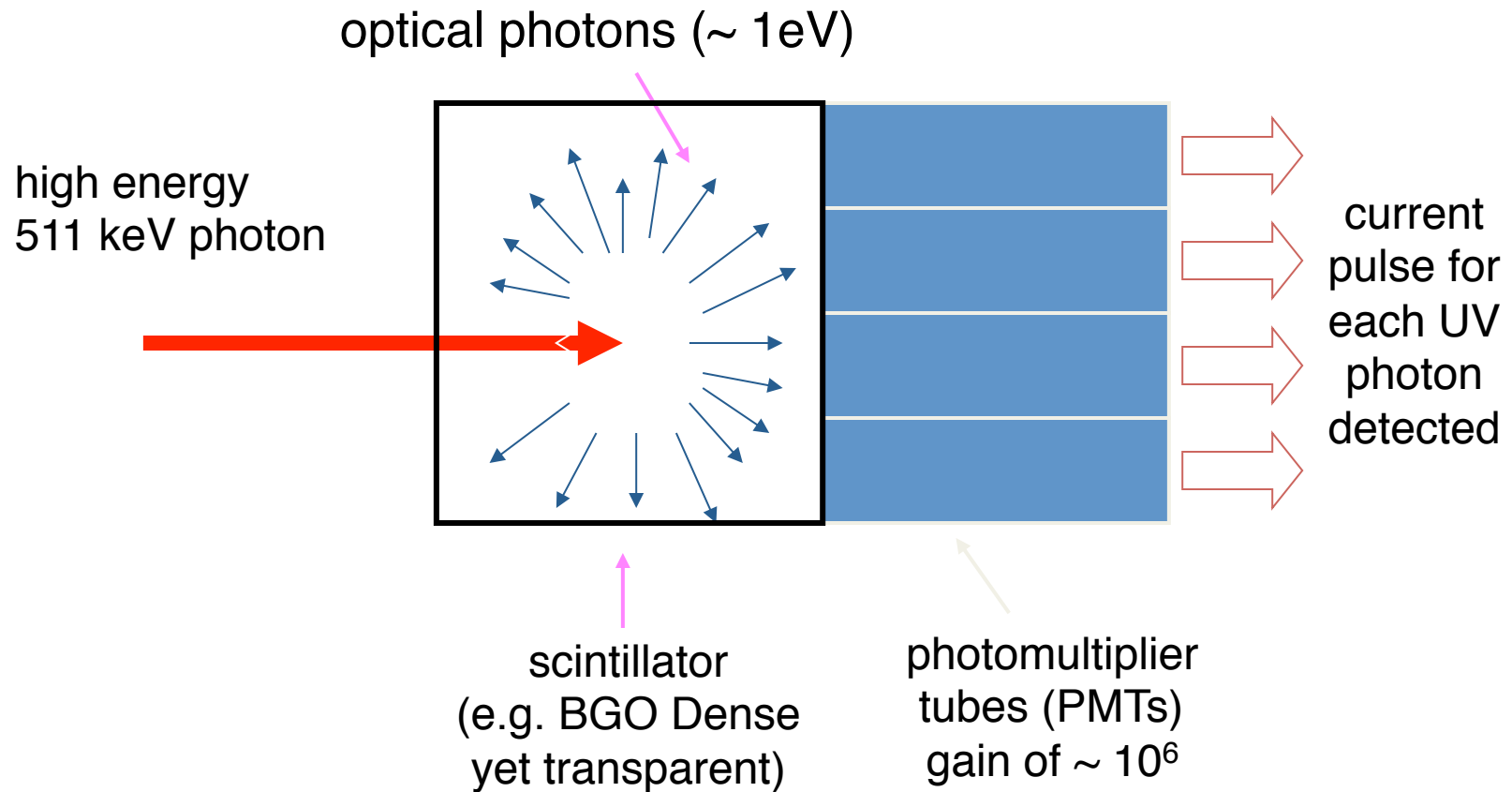
Medically Useful Positron Emitting Isotopes

Isotope	Half life (min)	Most probable energy (keV)	FWHM of positron range* in water (mm)
${}^{18}_9F$	109.7	203	0.102
${}^{82}_{37}Rb$	1.3	1384	0.169
${}^{11}_6C$	20.3	326	0.111
${}^{13}_7N$	10.0	432	0.142
${}^{15}_8O$	2.0	696	0.149

→ 90% of all clinical studies

* very long tails

Scintillation Detectors



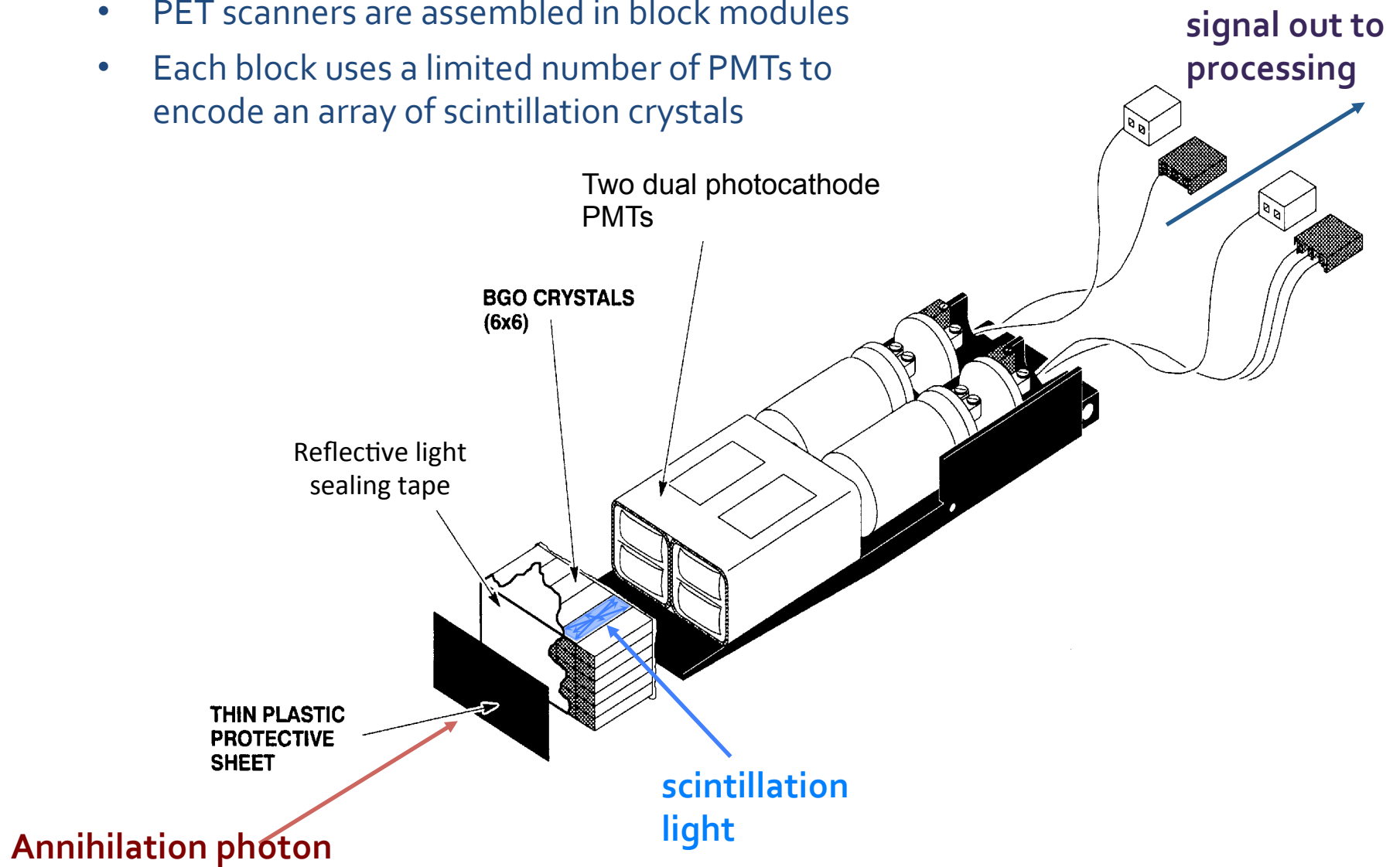
Scintillators tried in PET

Material	Density (g/cm ³)	Emission Maximum	Decay constant	Refractive index	Relative light output	Hygroscopic
Na(Tl)	3.67	415 nm	0.23 ms	1.83	100	yes
CsI(Tl)	4.51	550 nm	0.6/3.40 ms	1.79	45	no
CaF ₂	3.18	435 nm	0.84 ms	1.47	50	no
BaF ₂	4.88	315/220 nm	0.63 ms 0.80 ns	1.50 1.54	16 5	no
YAP(Ce)	5.55	350 nm	27.00 ns	1.94	35-40	no
GSO(Ce)	6.71	440 nm	30-60.00 ns	1.85	20-25	no
LSO(Ce)	7.40	420 nm	40.00 ns	1.82	75	no
BGO	7.13	480 nm	0.30 ms	2.15	15-20	no
CdWO ₄	7.90	470/540 nm	20/5.00 ms	2.30	25-30	no

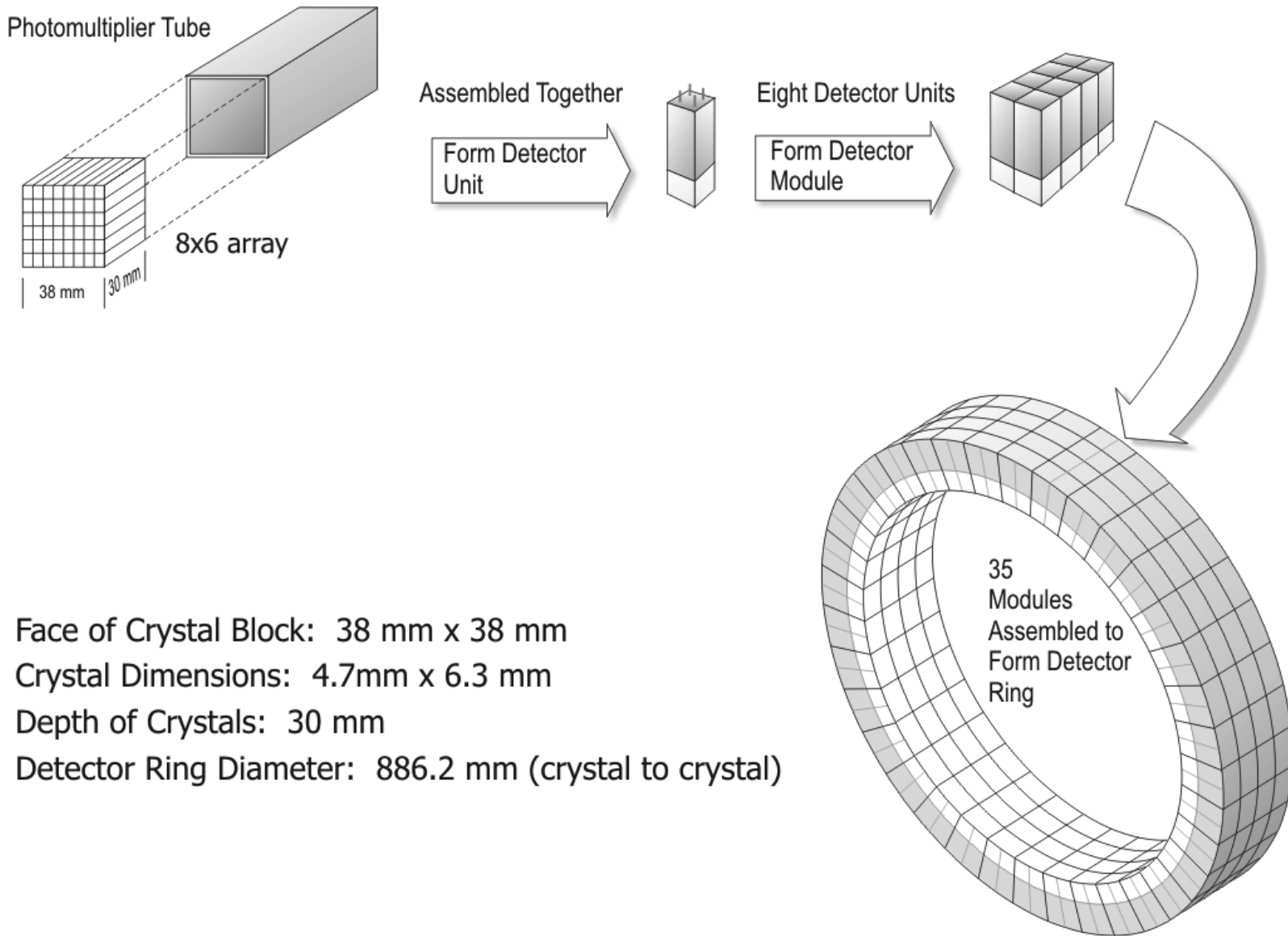
→ Used in commercial scanners

PET Detector Block

- PET scanners are assembled in block modules
- Each block uses a limited number of PMTs to encode an array of scintillation crystals



PET Scanner Detector Ring



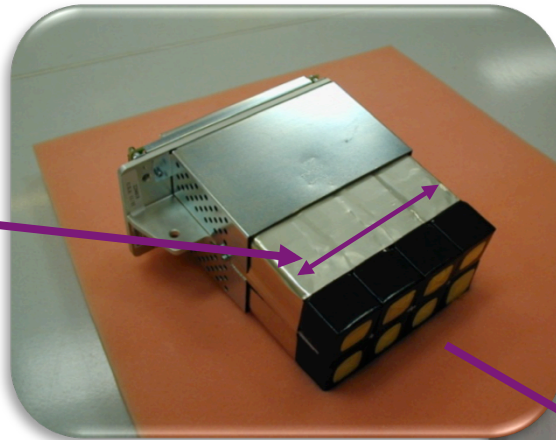
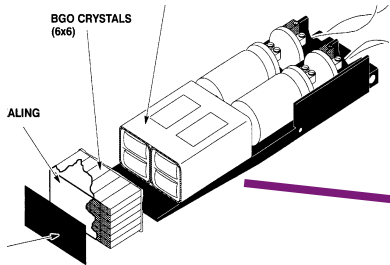
Face of Crystal Block: 38 mm x 38 mm

Crystal Dimensions: 4.7mm x 6.3 mm

Depth of Crystals: 30 mm

Detector Ring Diameter: 886.2 mm (crystal to crystal)

Block formation for a current PET scanner



Block matrix

6 x 8 crystals (axial by transaxial)

Each crystal:

6.3 mm axial

4.7 mm transaxial

Scanner construction

Axial:

4 blocks axially = 24 rings

15.7 cm axial extent

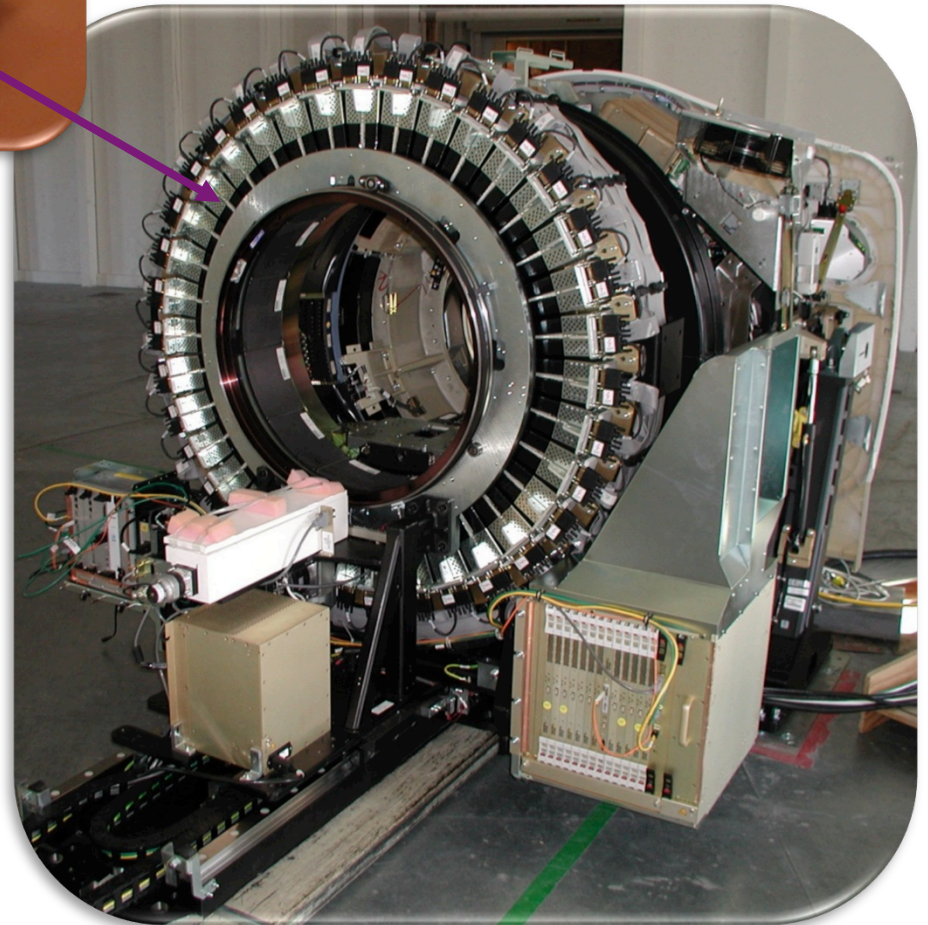
Transaxial:

70 blocks around = 560 crystals

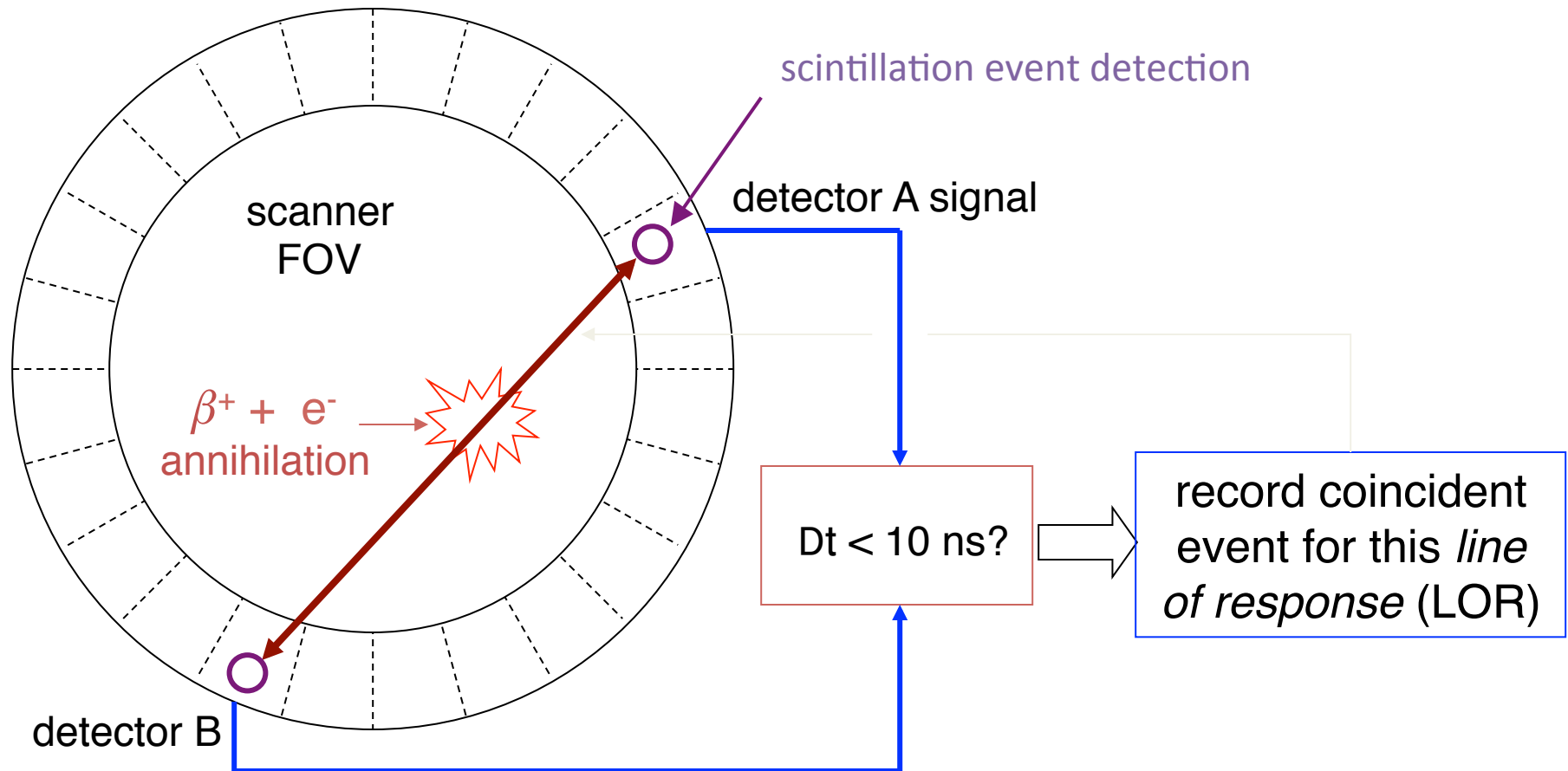
88 cm BGO ring diameter

70 cm patient port

13,440 individual crystals



Key feature of PET: Line of response collimation by coincidence timing

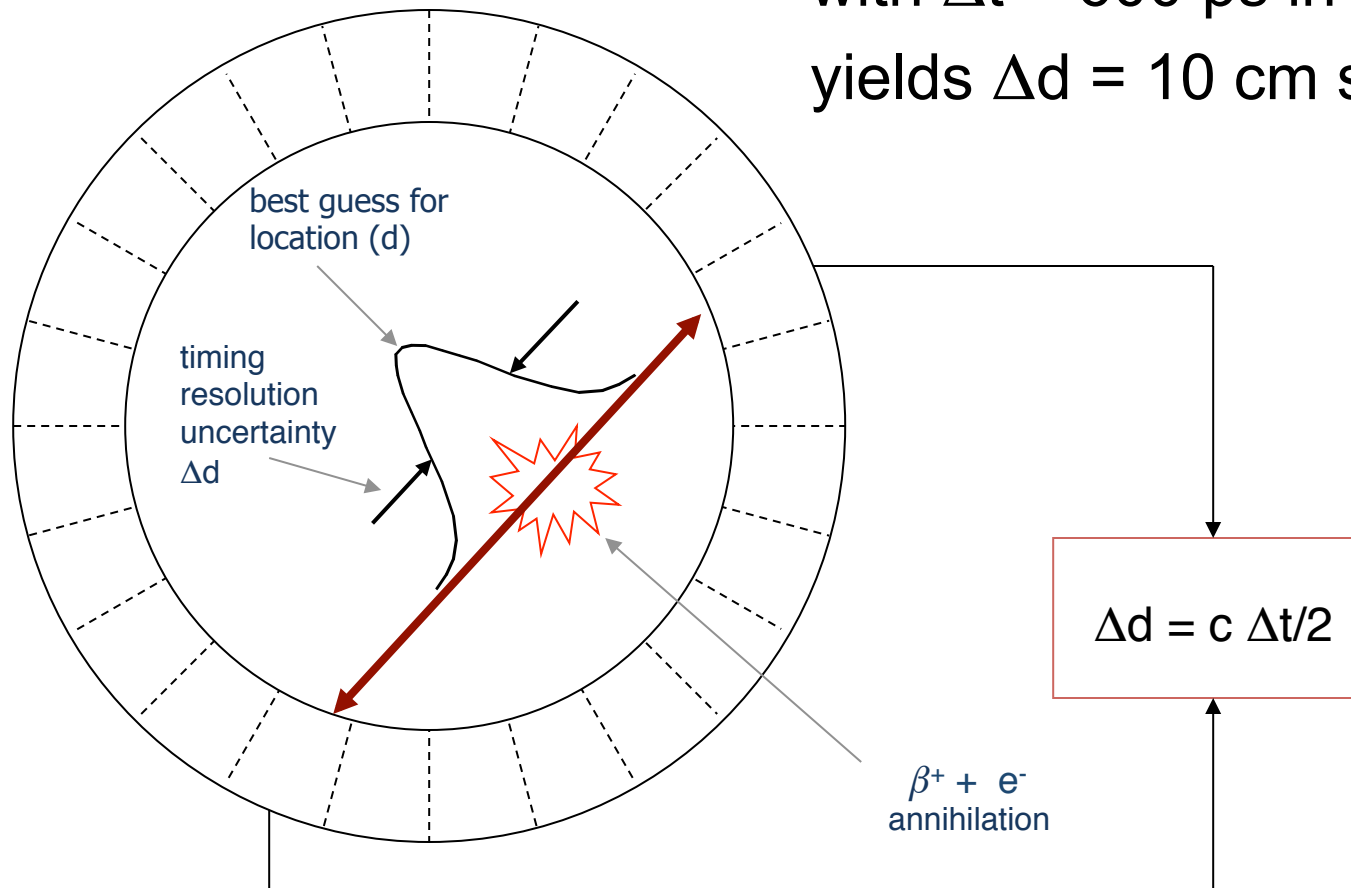


- In SPECT this is achieved through use of a collimator
- In CT the known geometry from source to detector is used

Time of Flight (TOF) PET/CT

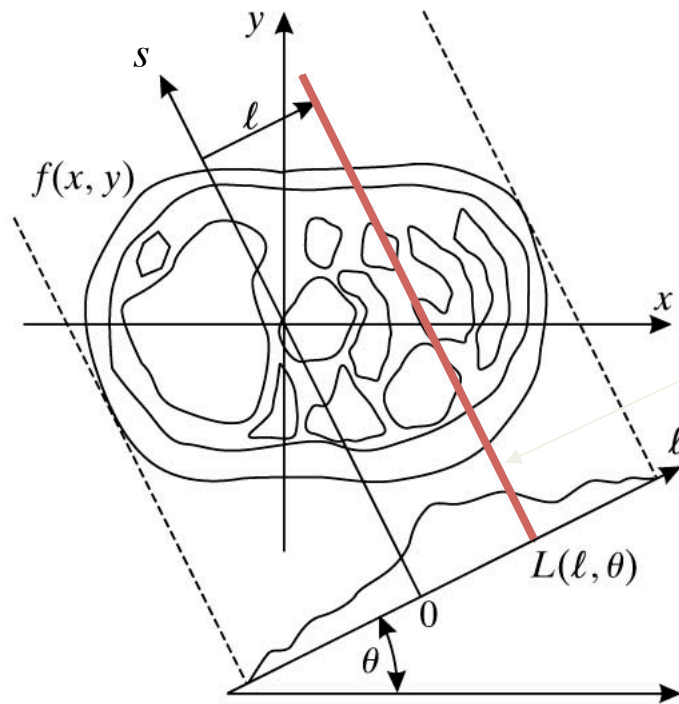
$$c = 3 \times 10^{10} \text{ cm/s}$$

with $\Delta t = 600 \text{ ps}$ in timing resolution
yields $\Delta d = 10 \text{ cm}$ spatial resolution



PET Imaging Equation

With enough coincident events for each *line of response*, we can approximate measures as *line-integral* data of the radioisotope concentration $A(x, y)$



$$\phi(l, \theta) = \int_{-\infty}^{\infty} A(x(s), y(s)) ds$$

The integral is along a line

$$L(l, \theta) = \{ (x, y) \mid x \cos \theta + y \sin \theta = l \}$$

Solving the PET Imaging Equation

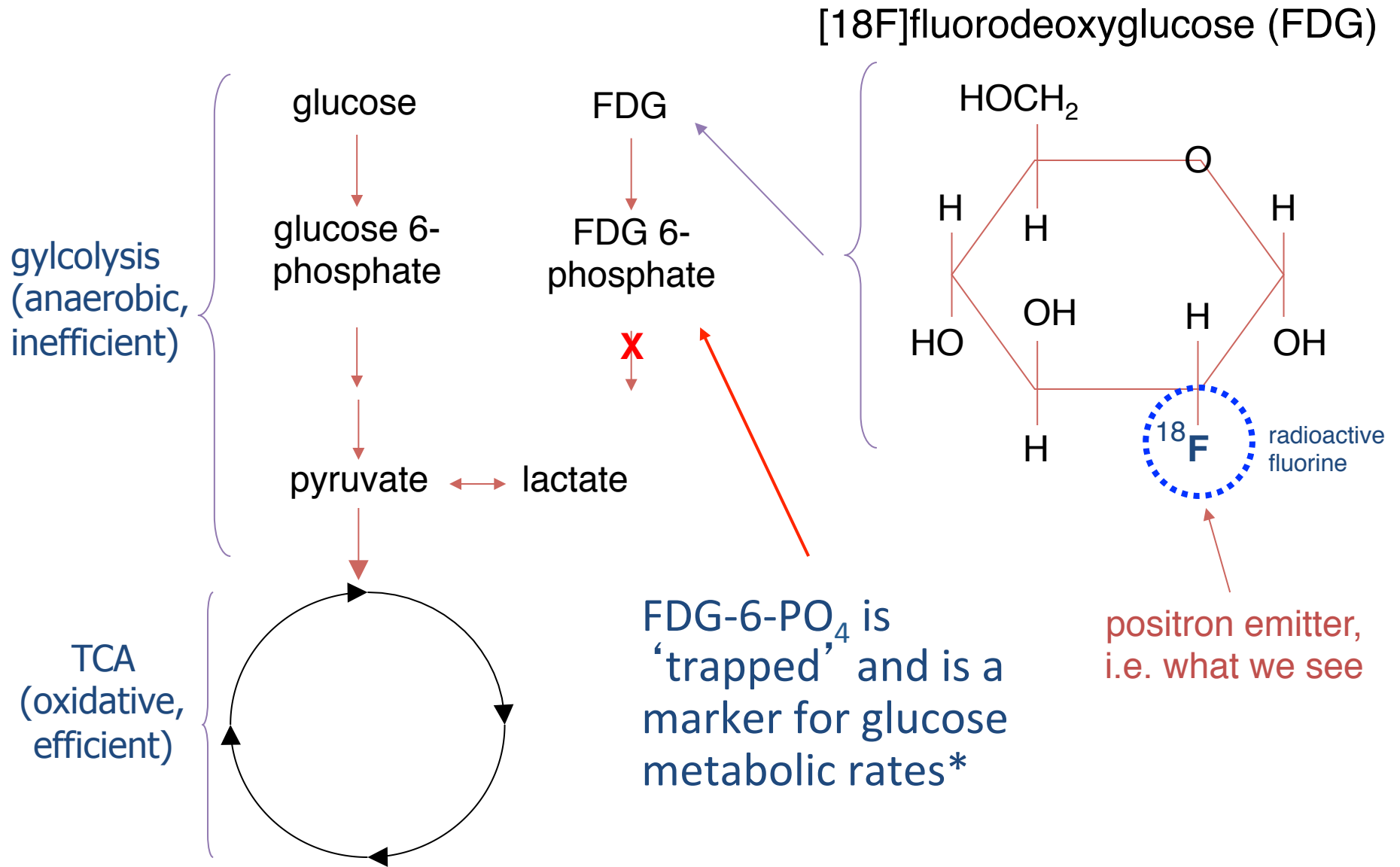
We have a simple 2D x-ray (Radon) transform, i.e. line integral, that can be exactly solved by filtered backprojection (FBP)

PET Imaging equation $\phi'(l, \theta) = \int_{-\infty}^{\infty} A(x(s), y(s)) ds$

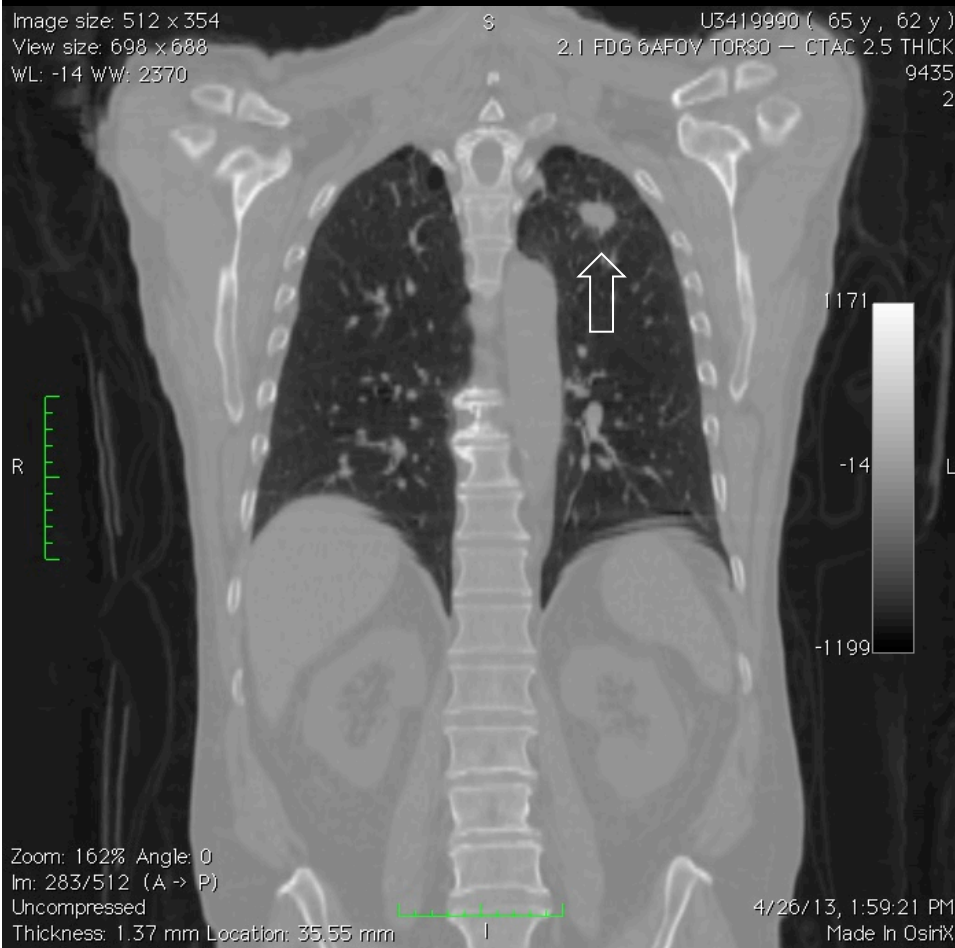
FBP solution $A(x, y) = \int_0^{\pi} \left[\int_{-\infty}^{\infty} |\rho| \Phi(\rho, \theta) e^{j2\pi\rho l} d\rho \right] d\theta$

where $\Phi(\rho, \theta) = \mathcal{F}_{1D} \{ \phi'(l, \theta) \}$

Typical use case: Glucose metabolism imaging



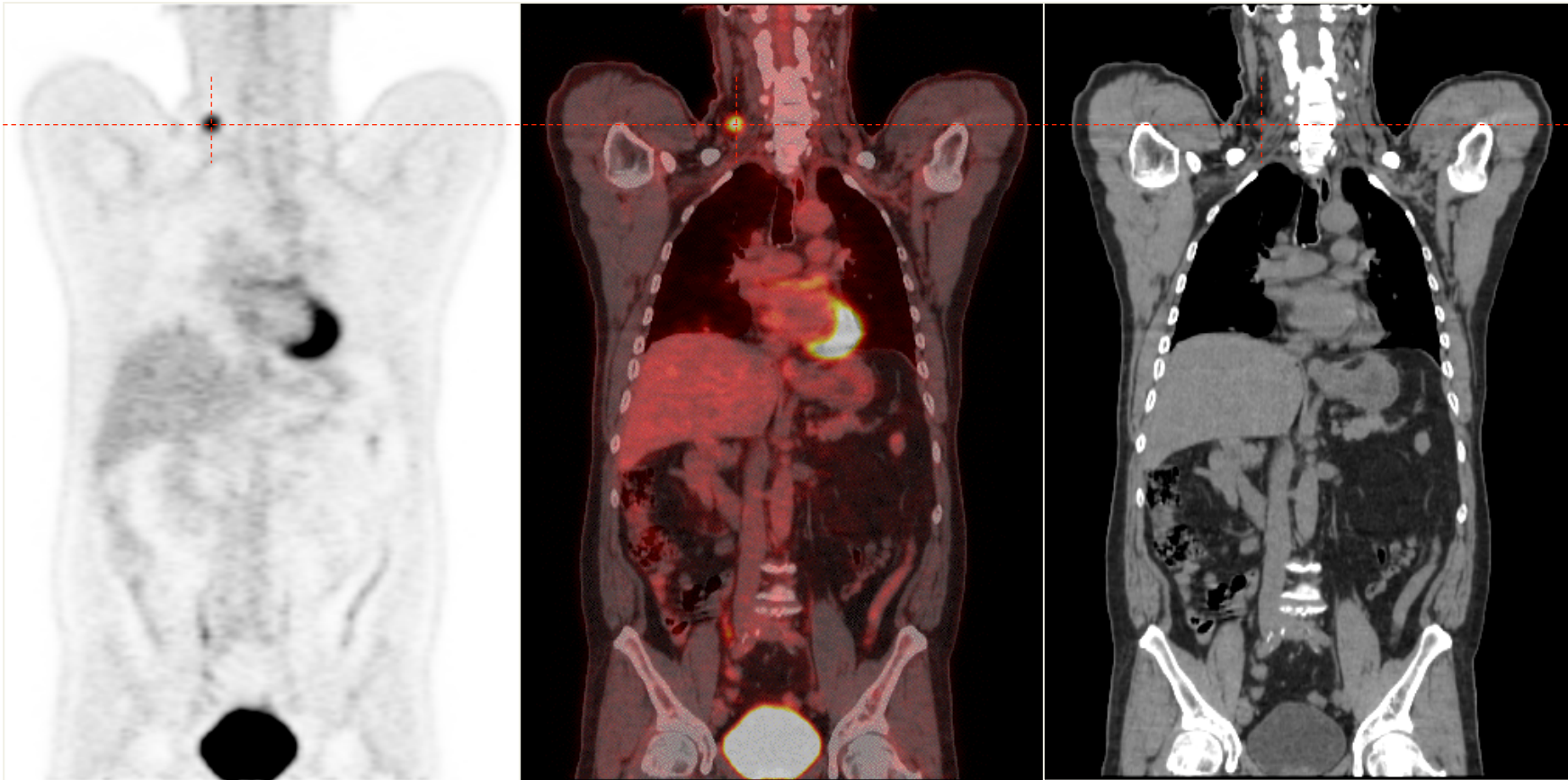
CT image showing suspicious nodule



PET image confirming cancer



Combined PET/CT imaging combines functional and anatomical imaging (like SPECT/CT)

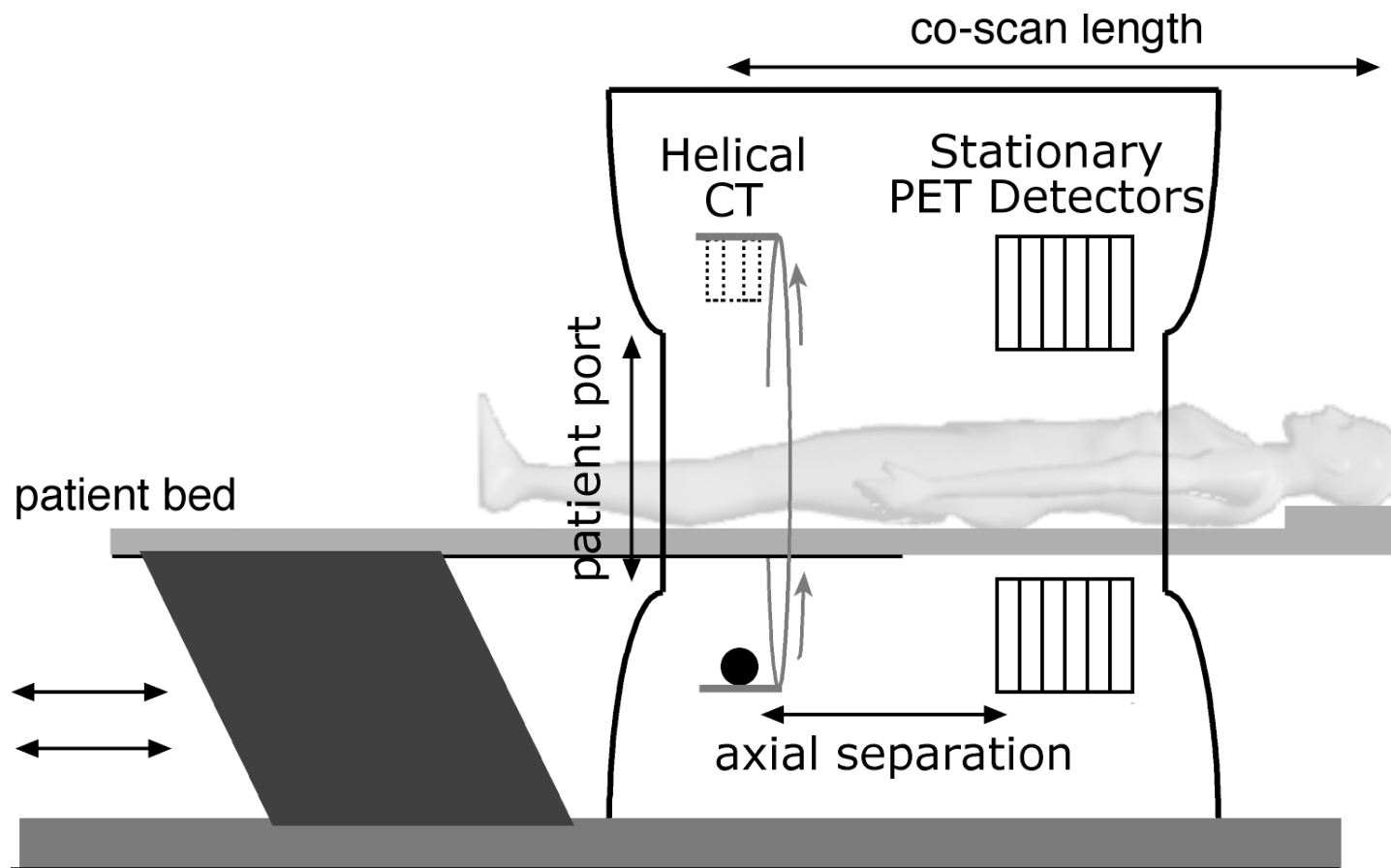


PET Image of Function

Function+Anatomy

CT Image of Anatomy

PET/CT scanner arrangement



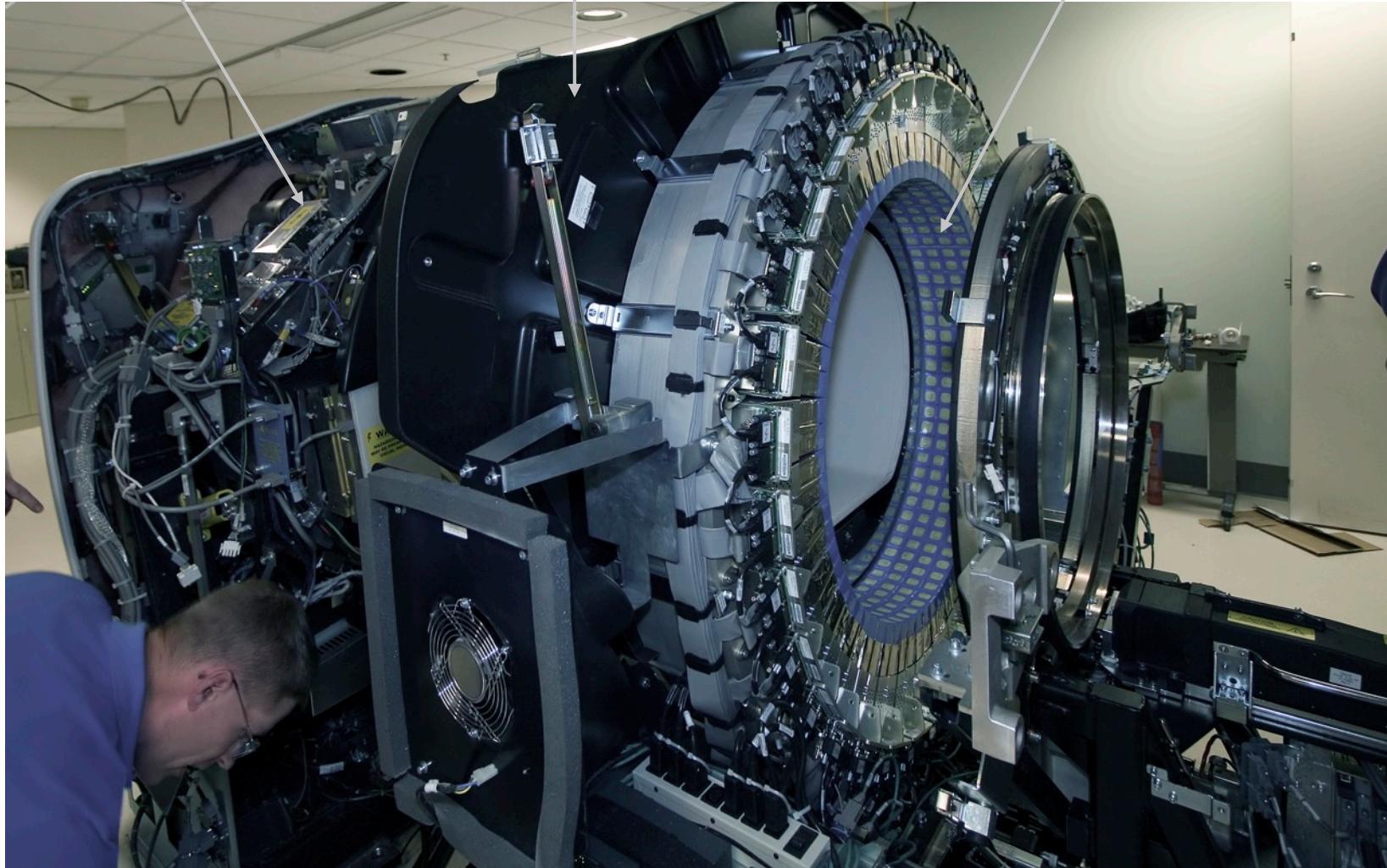
All 3 (couch, CT and PET) must be in accurate alignment

Commercial/Clinical PET/CT Scanner

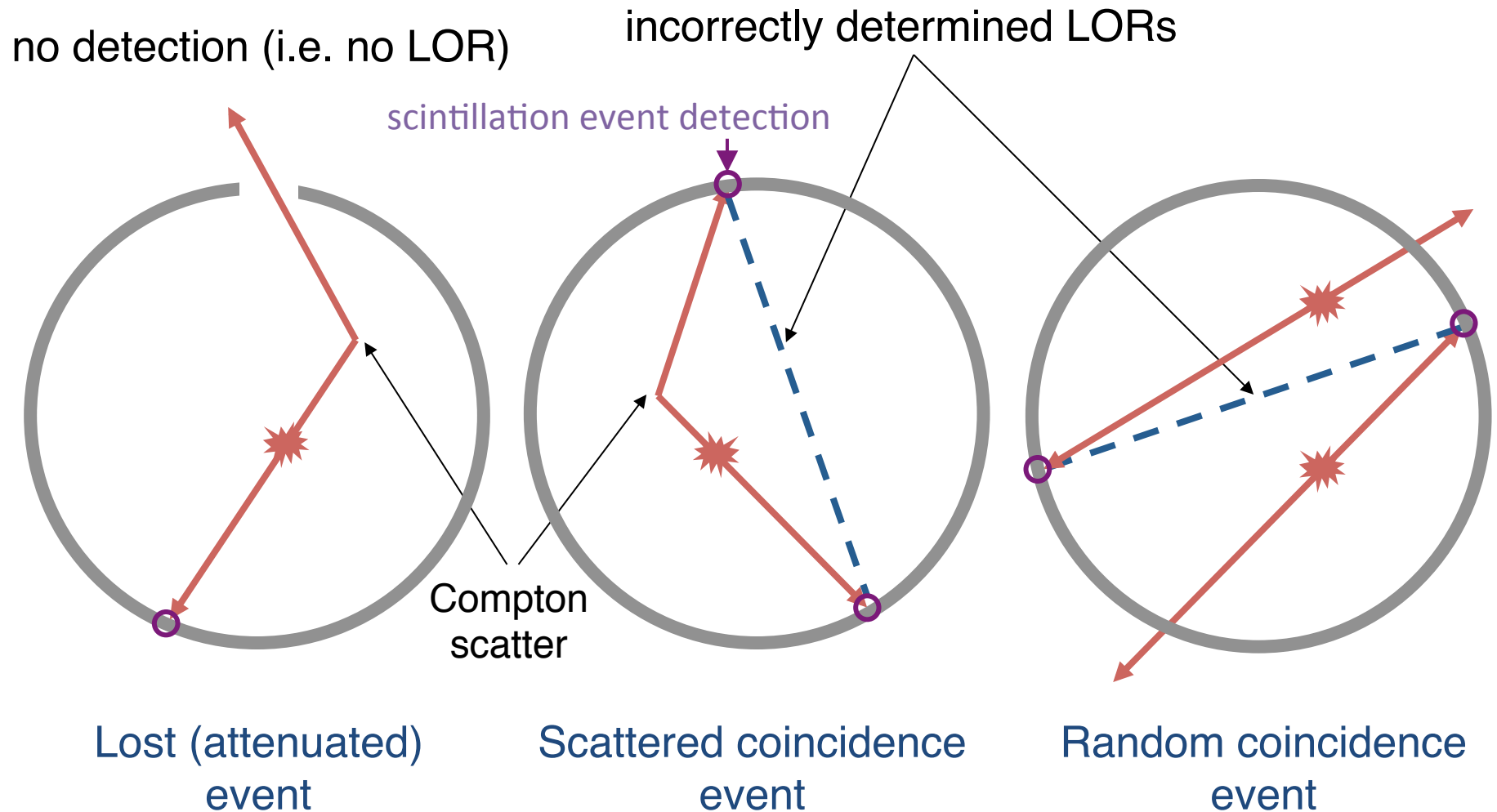
rotating CT system

thermal barrier

PET detector blocks



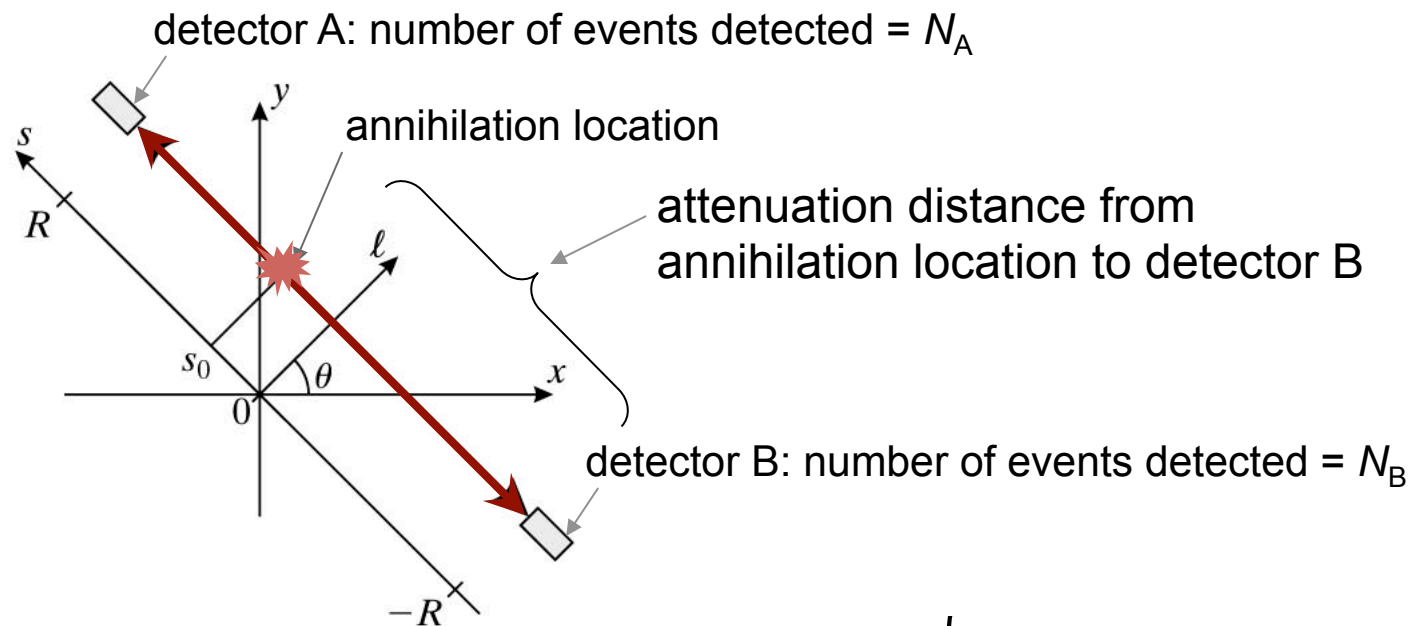
Confounding effects



Corrections have to be applied for these effects

Attenuation in PET Imaging

2 anti-colinear photons along the line of response (LOR)



photons detected from a single annihilation location at s_0

$$\begin{cases} N_A = N_0 \exp \left\{ - \int_{s_0}^R \mu(x(s'), y(s'); E) ds' \right\} \\ N_B = N_0 \exp \left\{ - \int_{-R}^{s_0} \mu(x(s'), y(s'); E) ds' \right\} \end{cases}$$

Attenuation in PET Imaging

Total number of annihilation photons arriving in coincidence N_C is N_0 (activity at s_0) reduced by the product of the attenuation factors

$$\begin{aligned} N_C &= N_0 \exp\left\{-\int_{s_0}^R \mu(x(s'), y(s'); E) ds'\right\} \exp\left\{-\int_{-R}^{s_0} \mu(x(s'), y(s'); E) ds'\right\} \\ &= N_0 \exp\left\{-\int_{-R}^R \mu(x(s'), y(s'); E) ds'\right\} \quad \text{key step is combining integrals} \end{aligned}$$

We can now allow for a distributed source of positrons along LOR

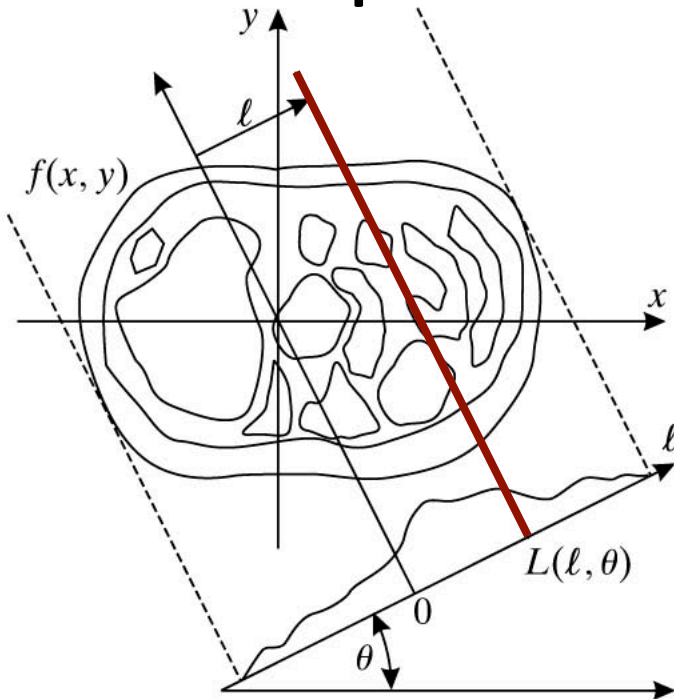
$$\phi(l, \theta) = K \int_{-R}^R A(x(s), y(s)) \exp\left\{-\int_{-R}^R \mu(x(s'), y(s'); E) ds'\right\} ds$$

not dependent on s so can take out of integral

even better, we now have attenuation as a simple multiplication

$$\phi(l, \theta) = K \int_{-R}^R A(x(s), y(s)) ds \cdot \exp\left\{-\int_{-R}^R \mu(x(s), y(s); E) ds\right\}$$

Comparison of Imaging Equations



x-ray transform integral along line

$$L(l, \theta) = \{(x, y) | x \cos \theta + y \sin \theta = l\}$$

With rotated coordinates (l, s)

$$x(s) = l \cos \theta - s \sin \theta$$

$$y(s) = l \sin \theta + s \cos \theta$$

CT
$$\phi(l, \theta) = \int_0^{E_{\max}} S_0(E) E \exp \left\{ - \int_{-R}^R \mu(x(s'), y(s'); E) ds' \right\} dE$$

SPECT
$$\phi(l, \theta) = \int_{-\infty}^R \frac{A(x(s), y(s))}{4\pi(s - R)^2} \exp \left\{ - \int_s^R \mu(x(s'), y(s'); E) ds' \right\} ds$$

PET
$$\phi(l, \theta) = K \int_{-R}^R A(x(s), y(s)) ds \cdot \exp \left\{ - \int_{-R}^R \mu(x(s), y(s); E) ds \right\}$$

Attenuation *Correction* in PET Imaging

We now have attenuation as a simple multiplication

$$\phi(l, \theta) = K \int_{-R}^R A(x(s), y(s)) ds \cdot \exp \left\{ - \int_{-R}^R \mu(x(s), y(s); E) ds \right\}$$

So is we can somehow measure attenuation along the LOR, i.e.

$$a(l, \theta) = \exp \left\{ - \int_{-R}^R \mu(x(s), y(s); E = 511 \text{keV}) ds \right\}$$

Then we can write

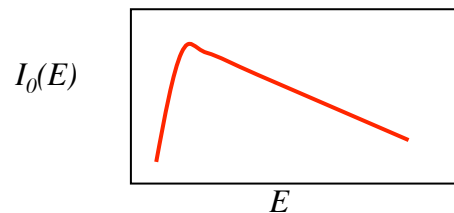
$$\phi'(l, \theta) = \frac{\phi(l, \theta)}{Ka(l, \theta)} = \int_{-\infty}^{\infty} A(x(s), y(s)) ds$$

Which we know how to solve for $A(x, y)$

Recall that $A(x, y)$ is the radiotracer (positron emitter) concentration that we want to know

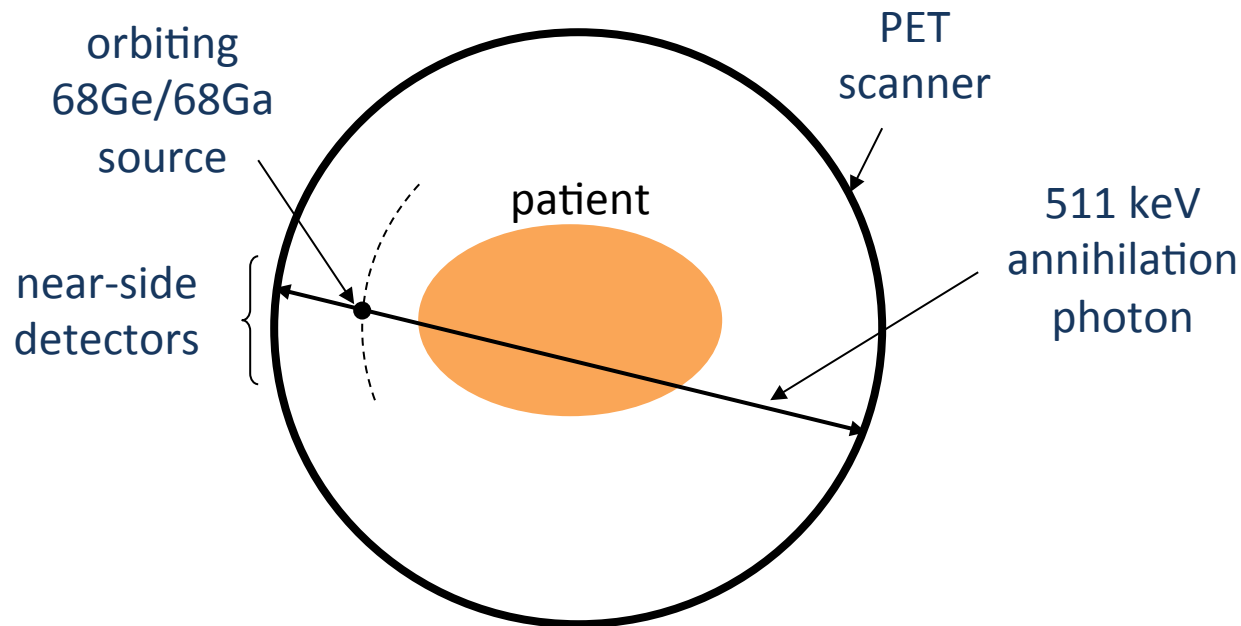
How to measure attenuation?

1. PET transmission source ($^{68}\text{Ge}/^{68}\text{Ga}$): Coincident annihilation photons (mono-energetic @ 511 keV), 265 day half life
2. X-ray CT scan: X-rays with a distribution of energies from ~30 to 130 keV (effective energy of ~70 keV)



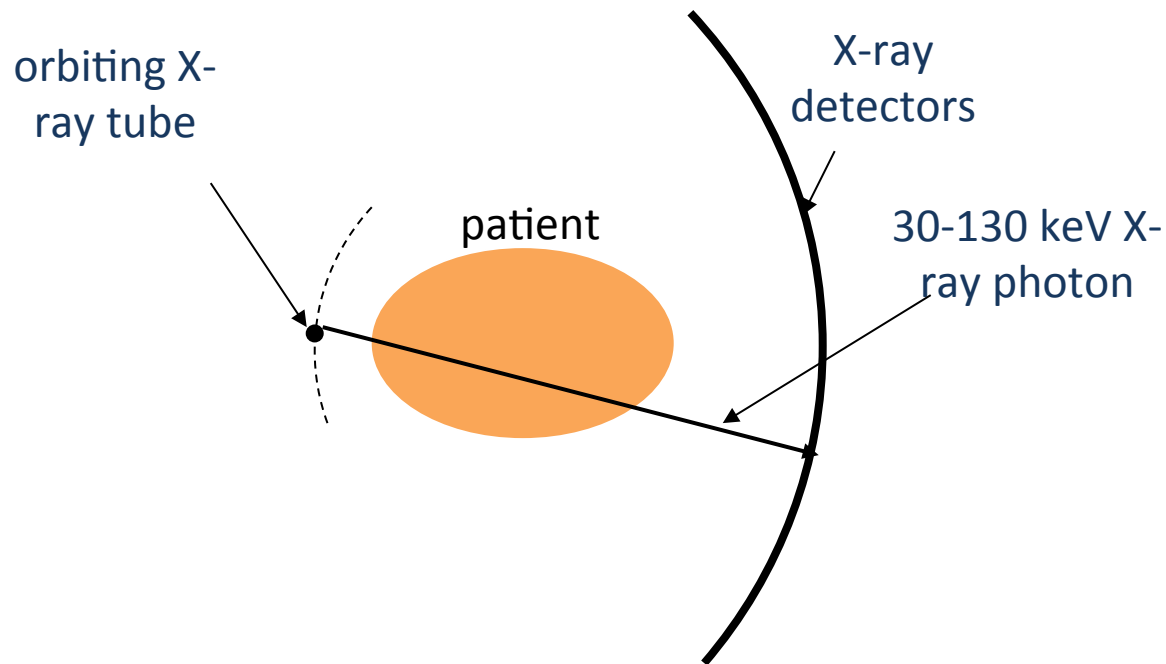
X-ray source spectra

PET attenuation imaging



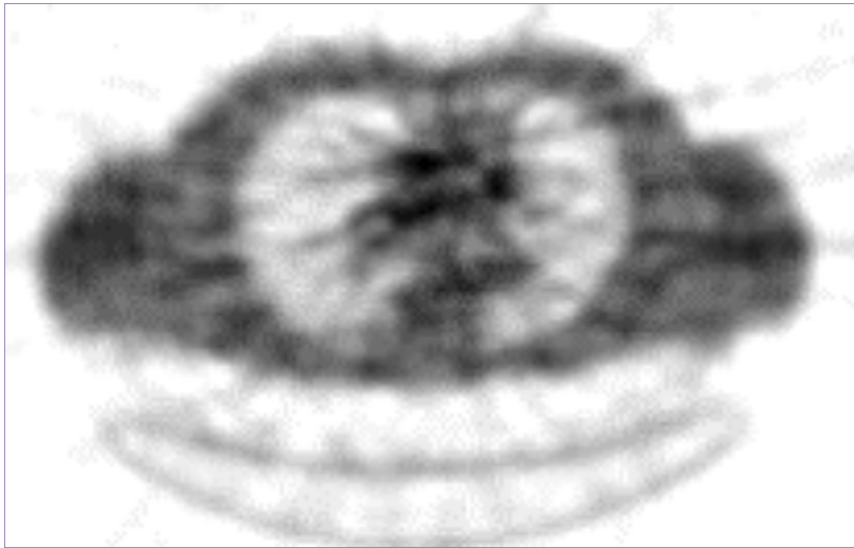
- $\mu(x,y)$ values are measured at desired energy of 511 keV
- Near-side detectors, however, suffer from deadtime due to high countrates
- Also subject to bias from emission photons from patient

X-ray CT attenuation imaging

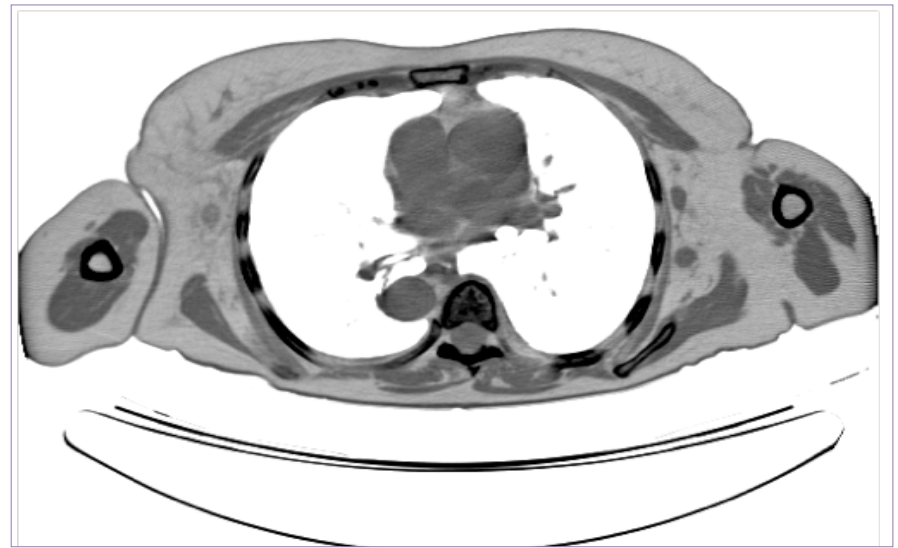


- $\mu(x,y,E)$ is measured as a weighted average from $\sim 30-130$ keV, so we need to convert to $t \mu(x,y,E=511\text{keV})$, potentially introducing bias
- Photon flux is very high, so very low noise and faster than PET transmission imaging

Comparison of attenuation imaging methods



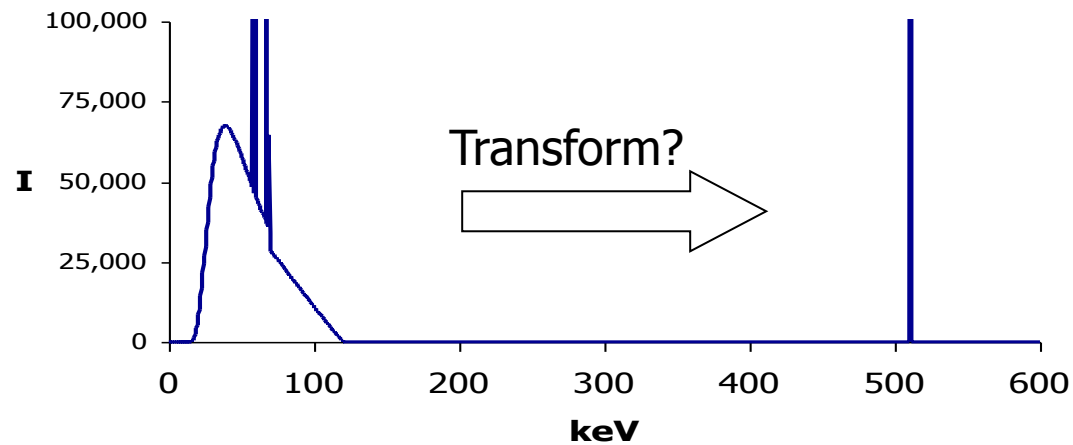
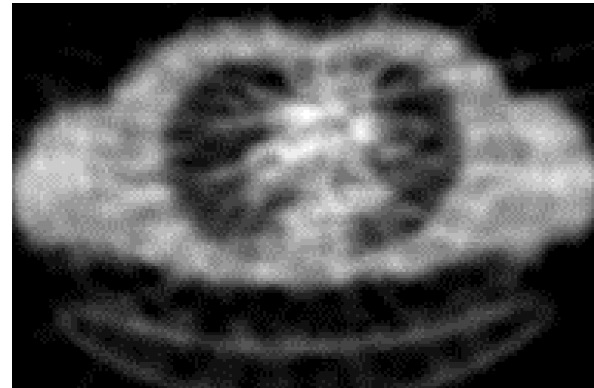
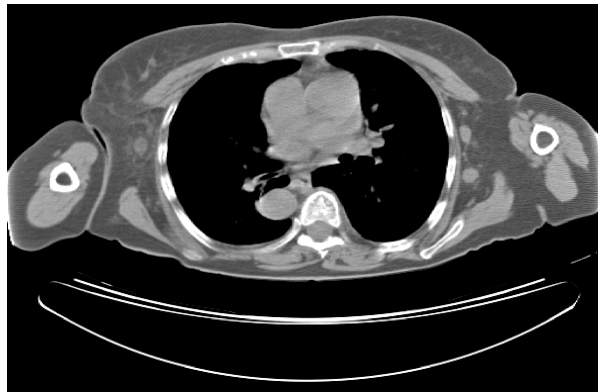
PET TX: 3min, $E = 511$ keV
unbiased estimate, high noise



X-ray CT TX: 20 s, $E = 30-120$ keV
biased estimate, low noise

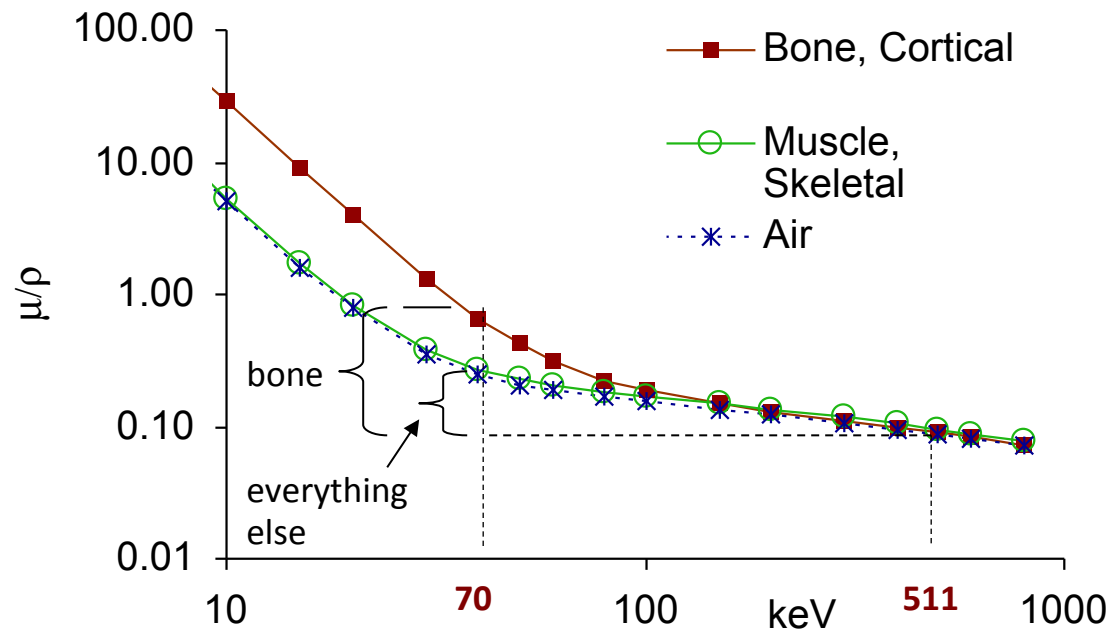
Due to diagnostic superiority of PET/CT, all PET scanners are really PET/CT scanners
so we can use CT for attenuation correction

CT-based Attenuation Correction



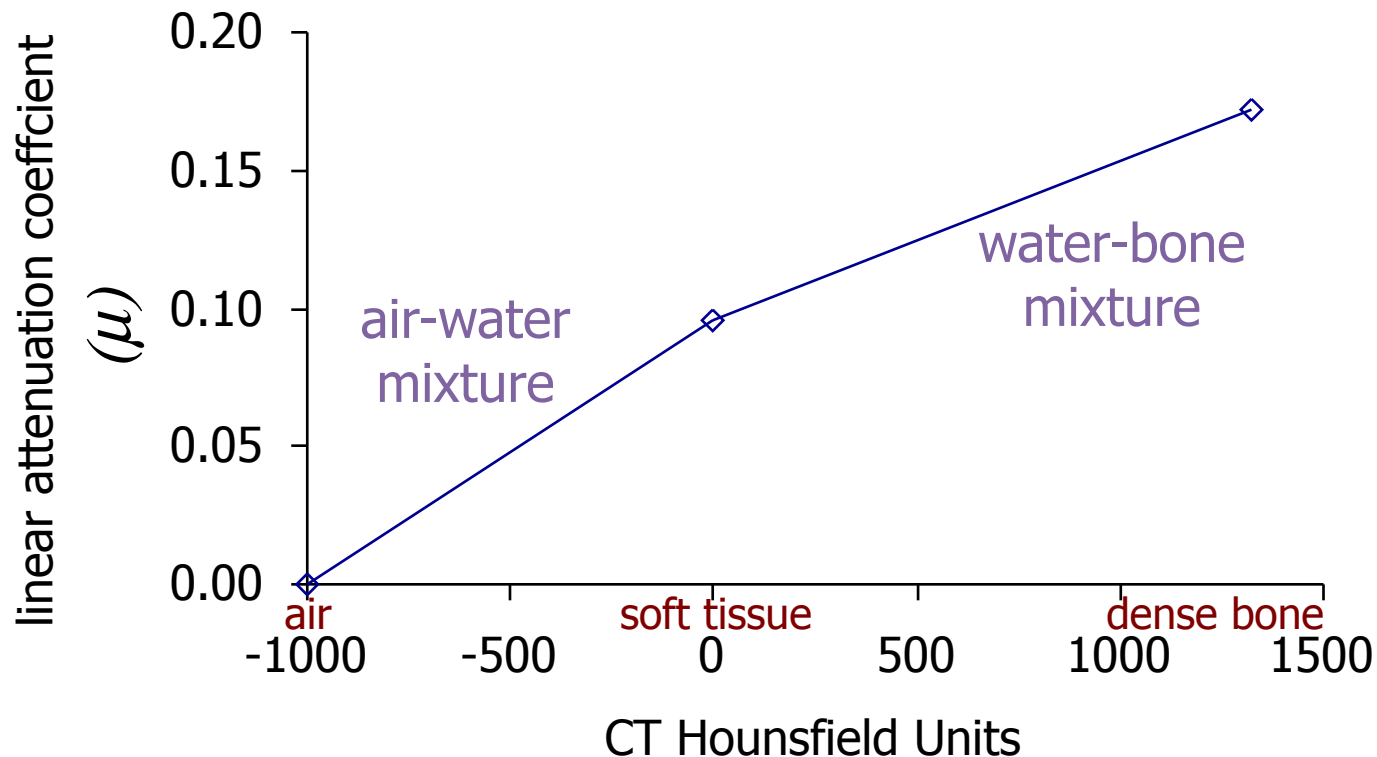
CT-based Attenuation Correction

- We use the fact that the mass-attenuation coefficient (μ/ρ) is similar for all non-bone materials since Compton scatter dominates for these materials
- Bone has a higher photoelectric cross-section due to calcium
- Can use two different scaling factors: one for bone and one for everything else



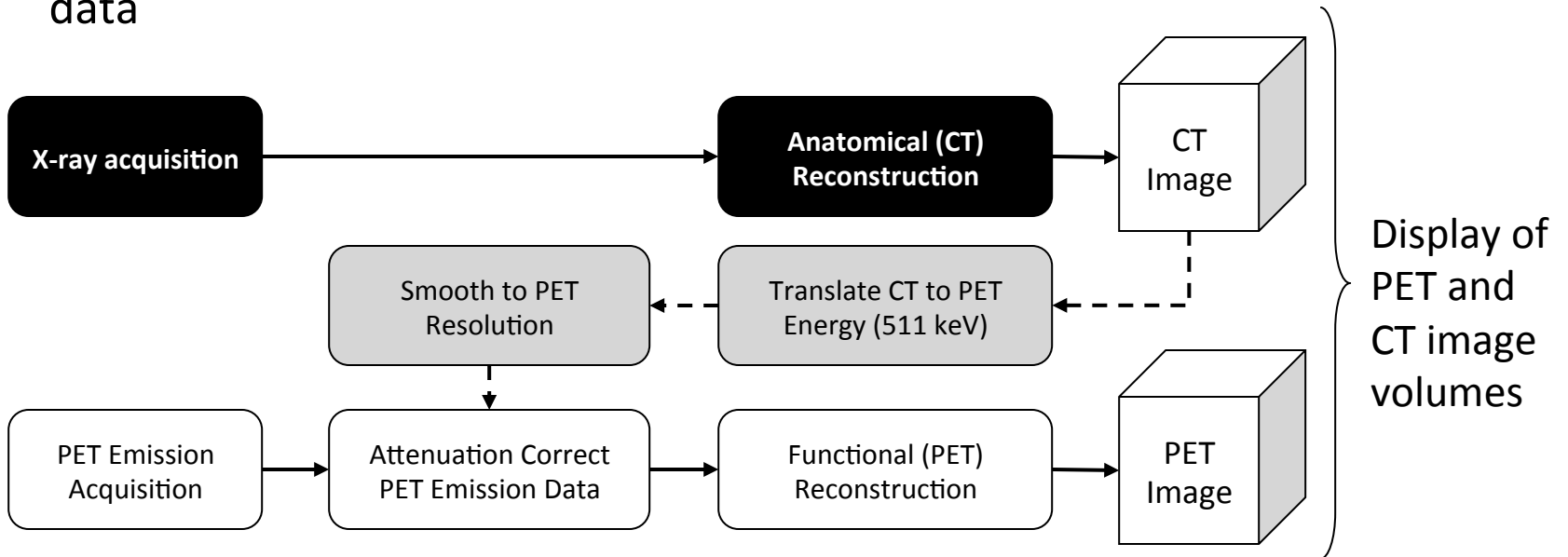
CT-based Attenuation Correction

- Bi-linear scaling methods apply different scale factors for bone and non-bone materials
- Should be calibrated for every kVp and/or contrast agent



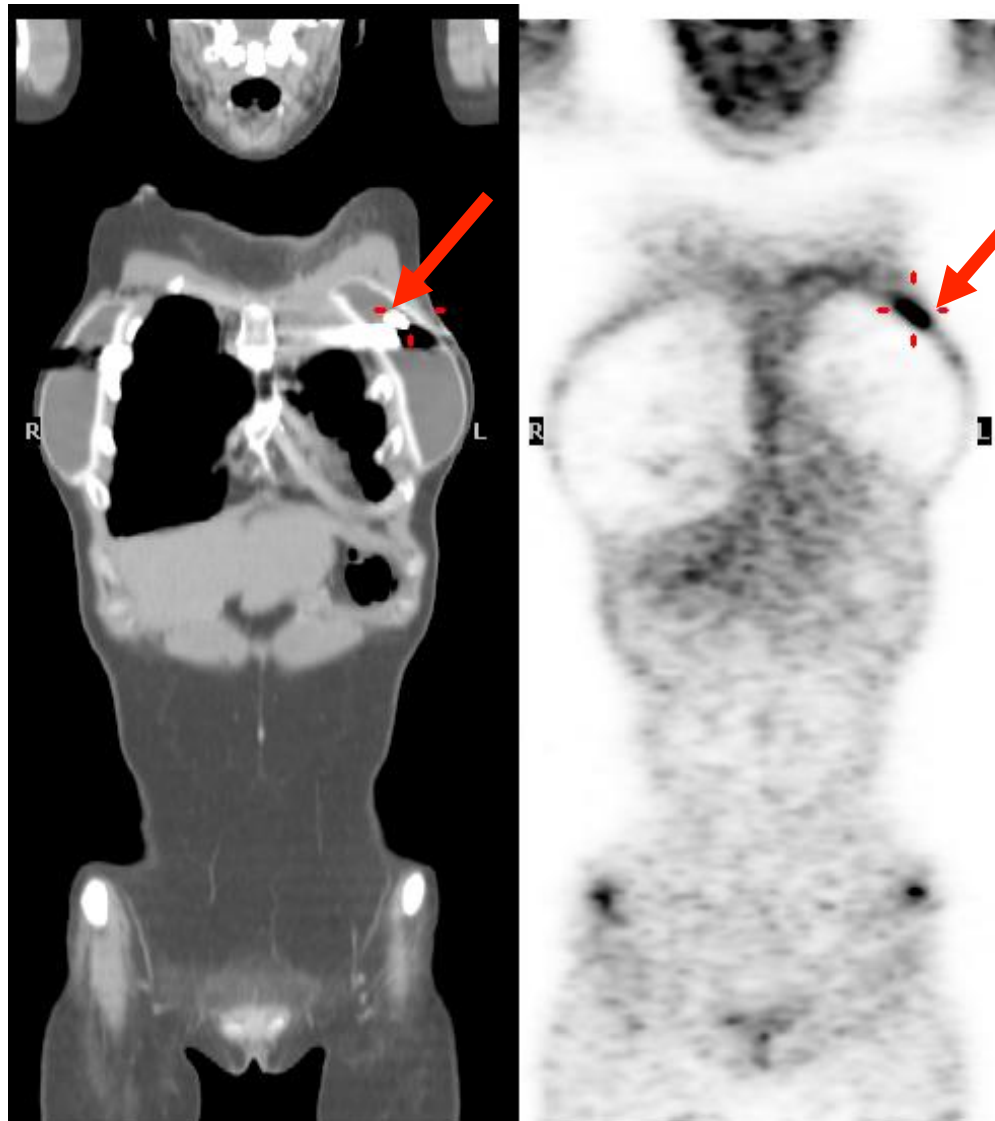
Data Flow and Processing

- CT images are also used for calibration (attenuation correction) of the PET data



- Note that images are not really fused, but are displayed as fused or side-by-side with linked cursors
- Note also that the CT is used for attenuation correction, thus a significant potential for error if there is a mis-alignment or inaccurate scaling

Material artifact: Metal Clip



Artifact

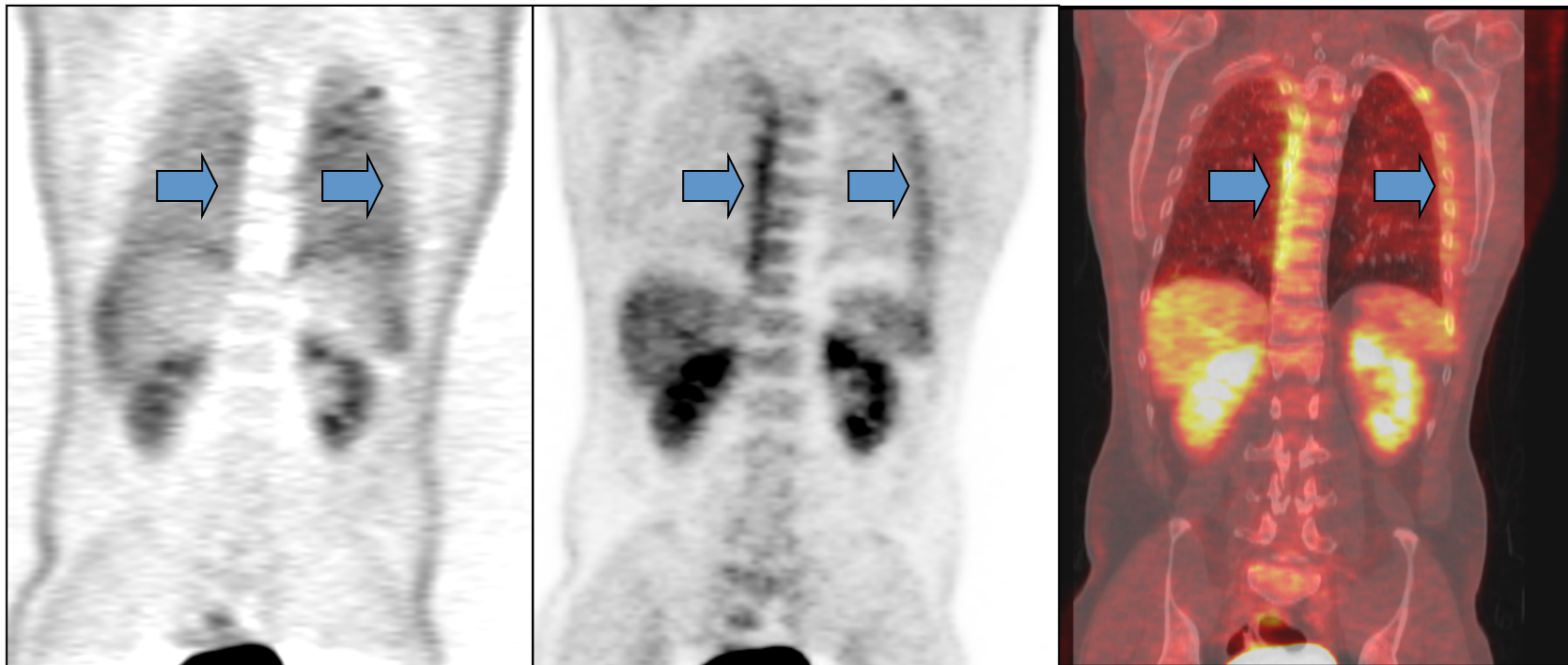
CT

PET with CTAC

*Courtesy O Mawlawi
MDACC*

Positional artifact: Patient and/or bed shifting

Large change in attenuation at lung boundaries, so very susceptible to errors

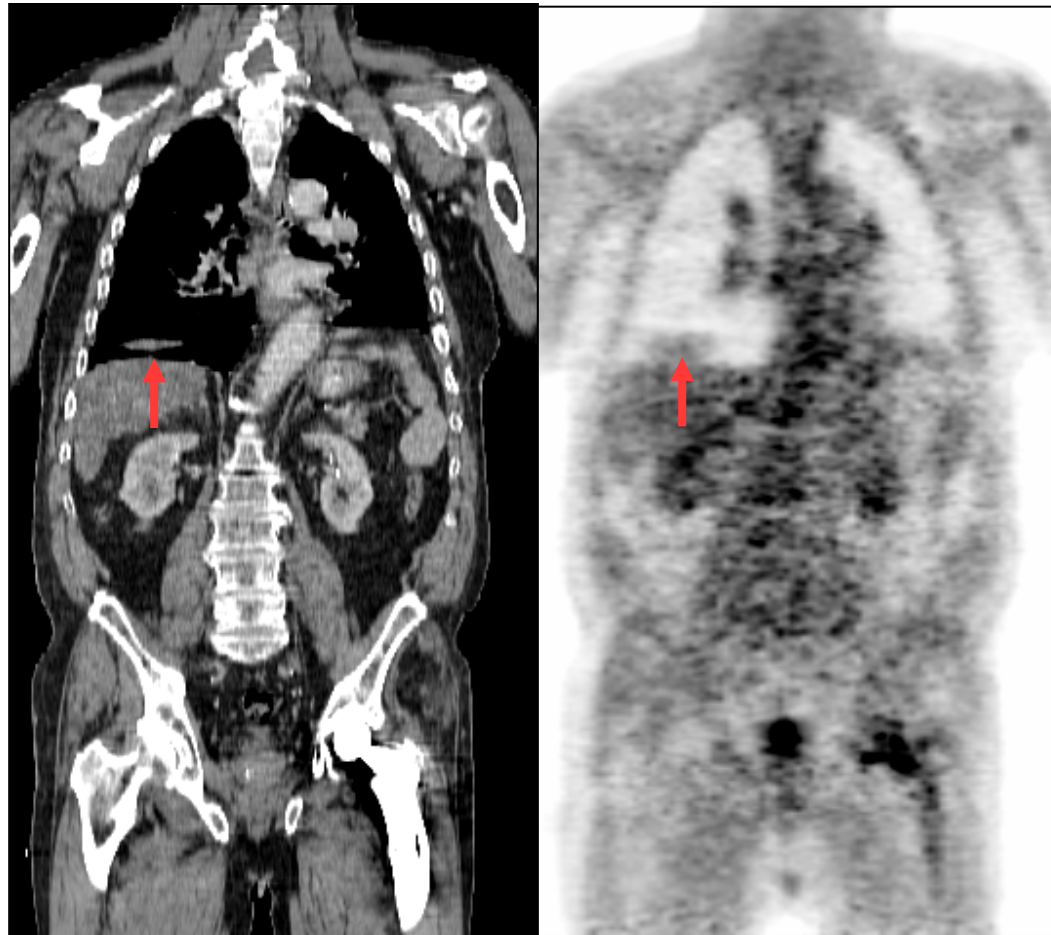


PET image without attenuation correction

PET image with CT-based attenuation correction

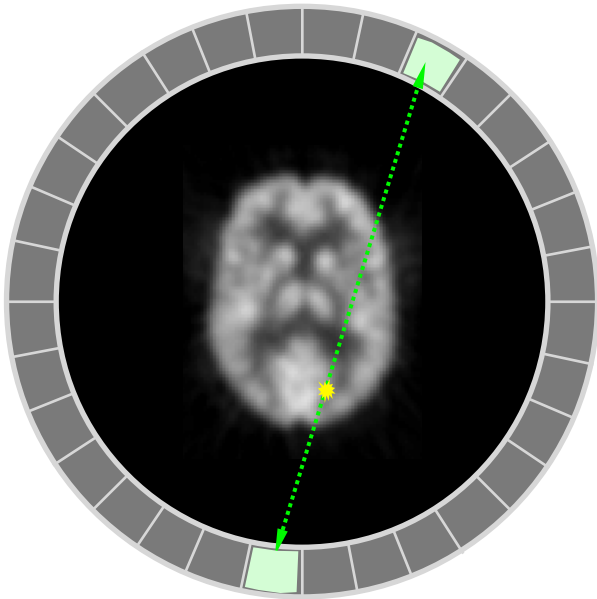
PET image fused with CT

Respiratory Motion Artifacts

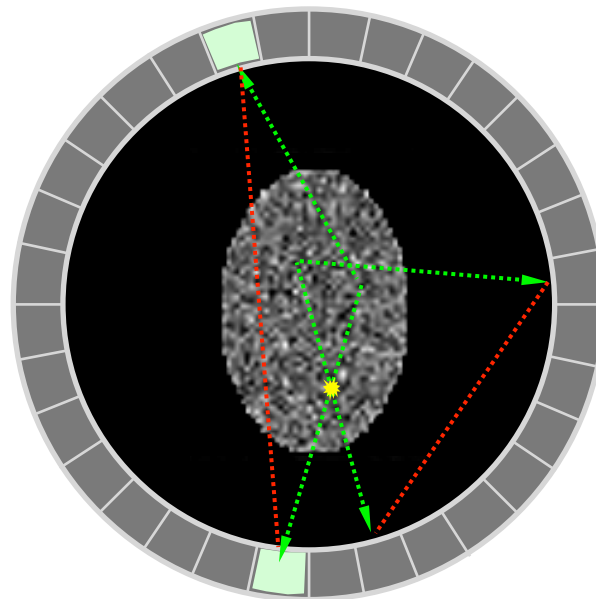


Attenuation artifacts can dominate true tracer uptake values

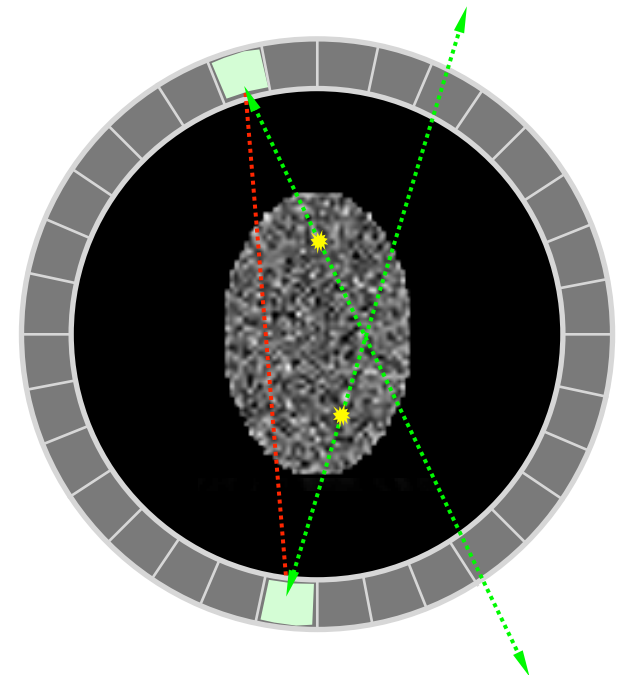
PET Signal, Bias, and Noise



True coincidence (T):
line integral signal we
want but effected by
photon counting noise



Scattered coincidence (S):
bias and noise added to
data



Random coincidence (R):
different type of bias
added to data, also noise

Components of measured PET data

$$P = \wp\{aT\} + \wp\{S\} + \wp\{R\}$$

Measured Projections attenuated True Signal bias from Scatter bias from Random events

$$T = \phi'(l, \theta) = \int_{-\infty}^{\infty} A(x(s), y(s)) ds$$

$\wp\{x\}$, Poisson random process with mean x

- If we can estimate S and R as S' and R' (how is beyond scope of this lecture) then:

$$\int_{-\infty}^{\infty} A(x(s), y(s)) ds \simeq \frac{1}{a}(P - S' - R')$$

- We can solve this with FBP

Signal to Noise Ratio (SNR)

- Signal is the true counts T
- The noise is the total noise in the data P
- We can estimate noise by realizing that photon counting is a Poisson process, so the variance is equal to the mean

$$\sigma(P) = \sqrt{T + S + \alpha R}$$

α depends on randoms estimation method

$$\text{SNR} = \frac{T}{\sigma(P)} \approx \frac{T}{\sqrt{T + S + \alpha R}} = \sqrt{\text{NEC}}$$

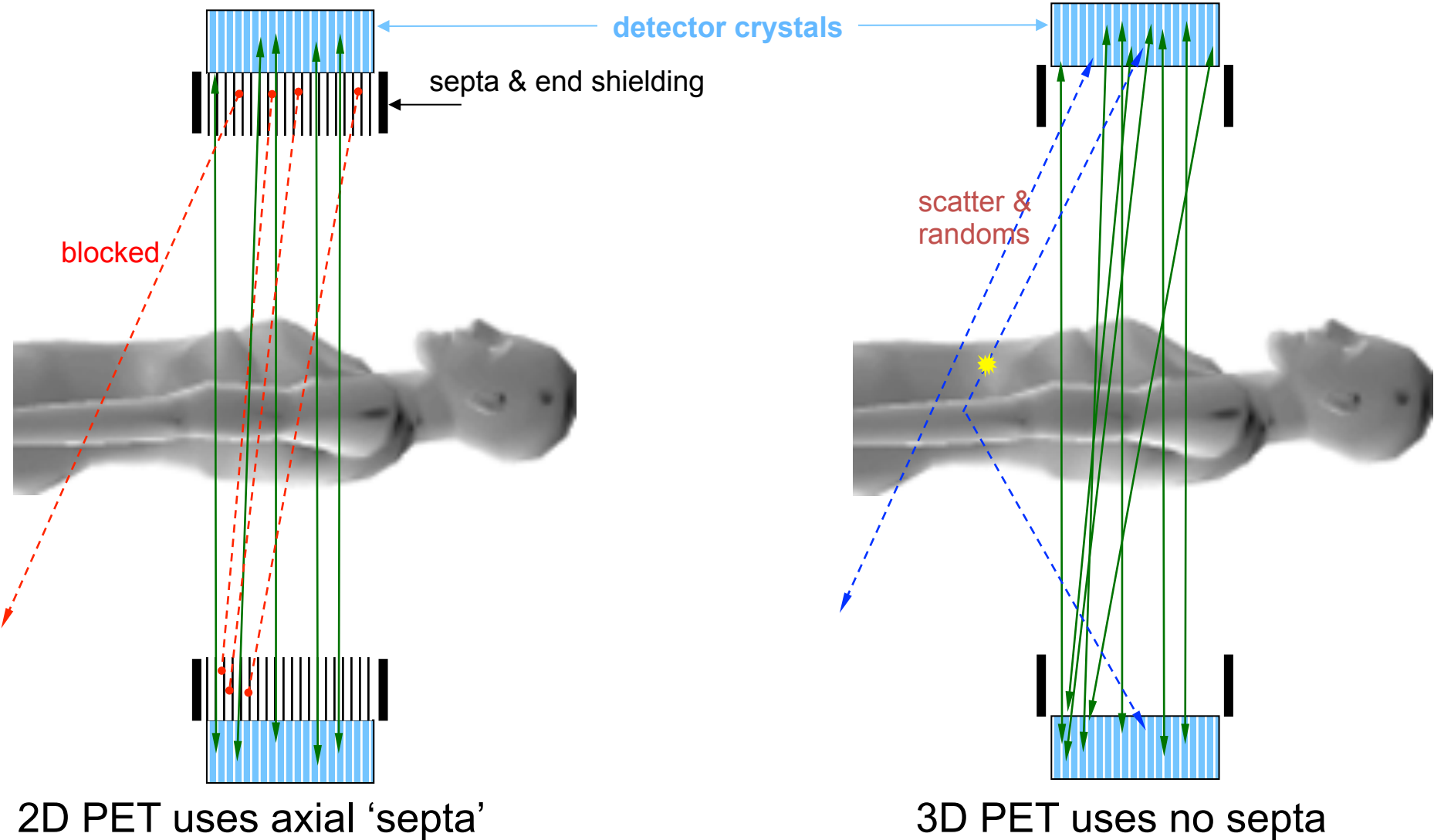
NEC is called the 'noise equivalent count' rate, i.e. the useful count rate

$$\text{NEC} = \frac{T^2}{T + S + \alpha R} < T$$

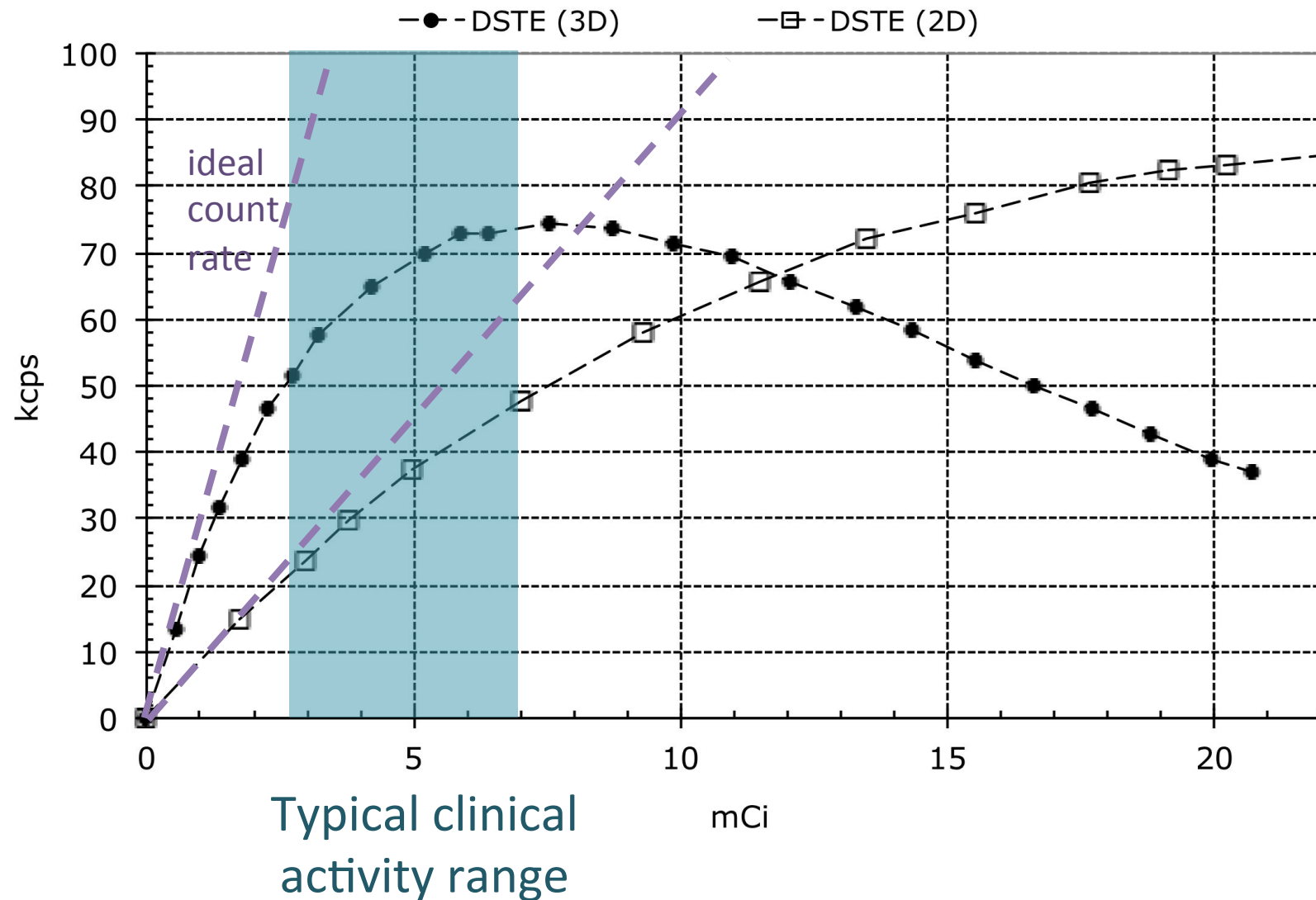
The NEC is always less than T

PET Acquisition: 2D vs. 3D Mode

3D mode typically has higher NEC than 2D mode for activity levels of interest



Impact of 3D and 2D mode on NEC rates



Spatial Resolution component of SNR

- Positron Physics
 - Positron Range
 - Photon Non-collinearity
- Detectors
 - Response function
- Ring Geometry
 - Non-uniform LOR sampling
 - Depth-of-interaction
- Reconstruction Filters

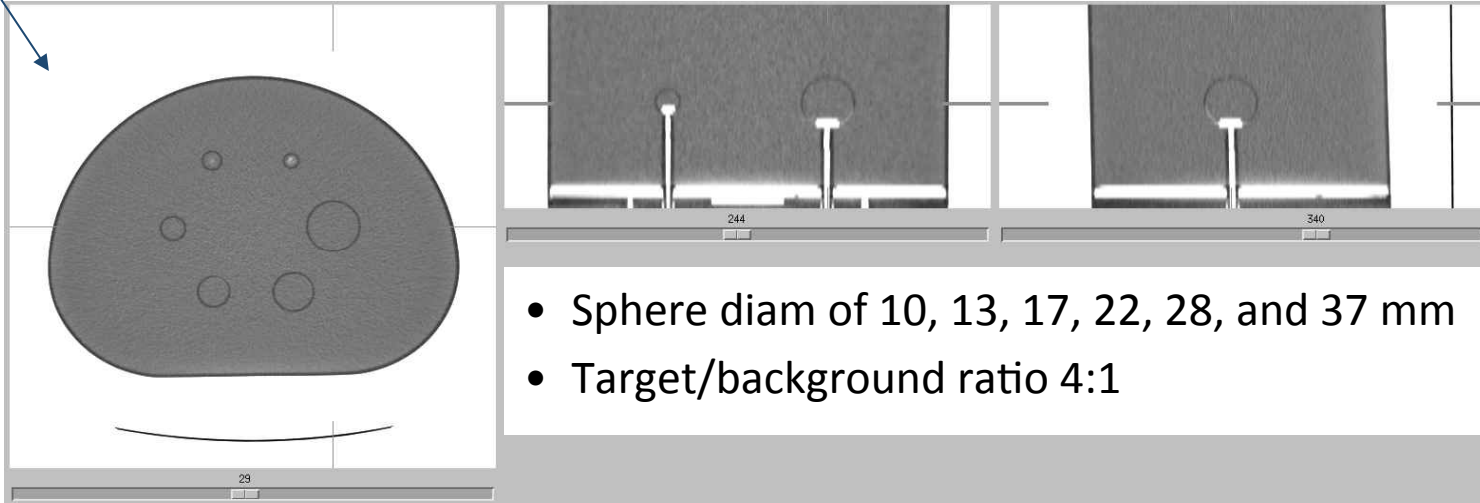
Resolution components add in quadrature

$$R_{system} = \sqrt{R_{pos.phys.}^2 + R_{det}^2 + R_{sampl}^2 + R_{recon}^2}$$

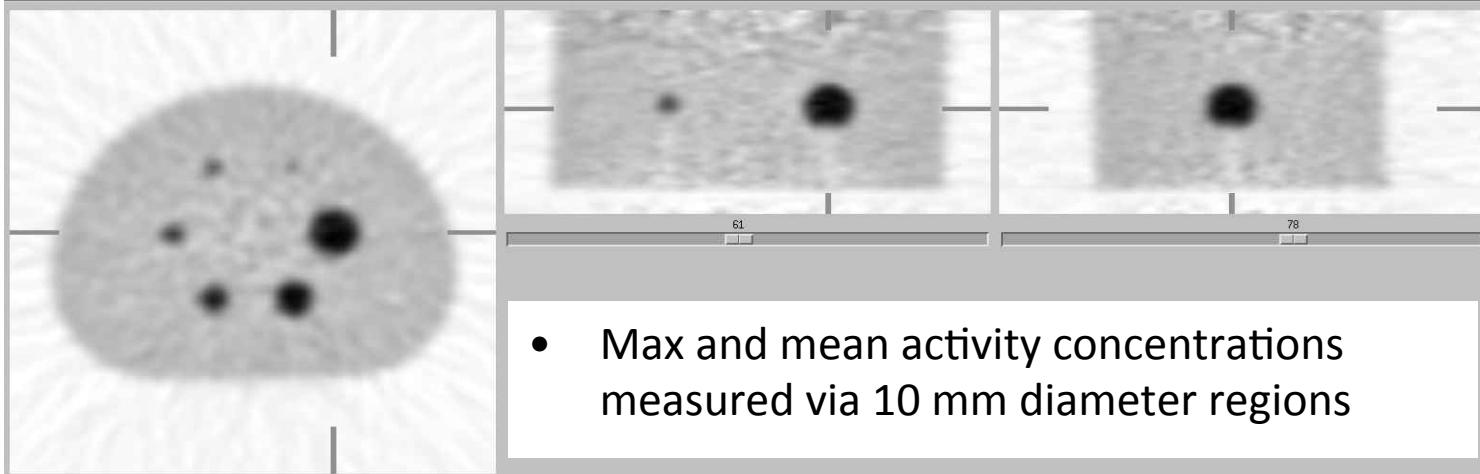
Size-Dependent Resolution Losses

20 x 30 cm, similar to abdominal x-section

CT

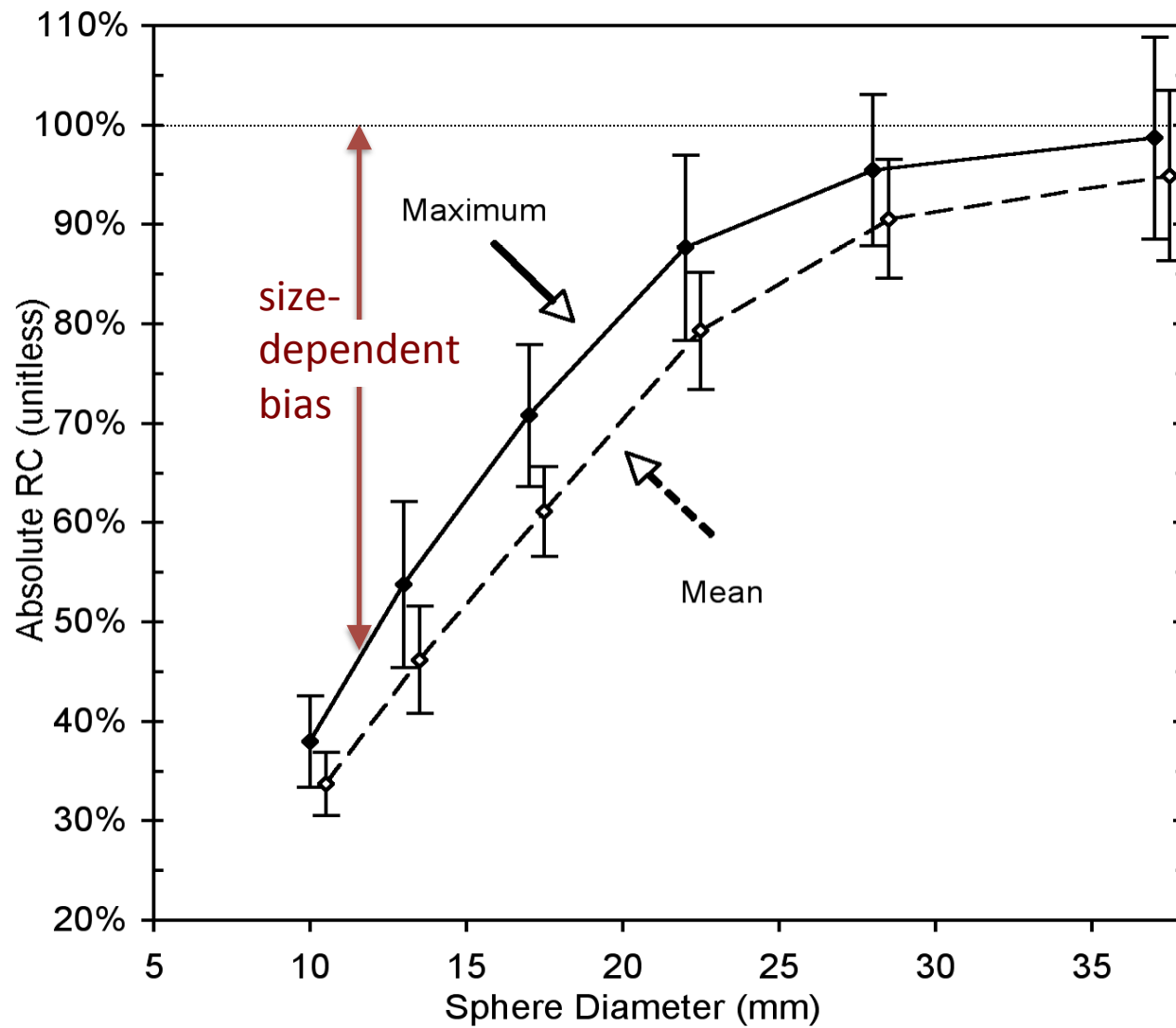


PET



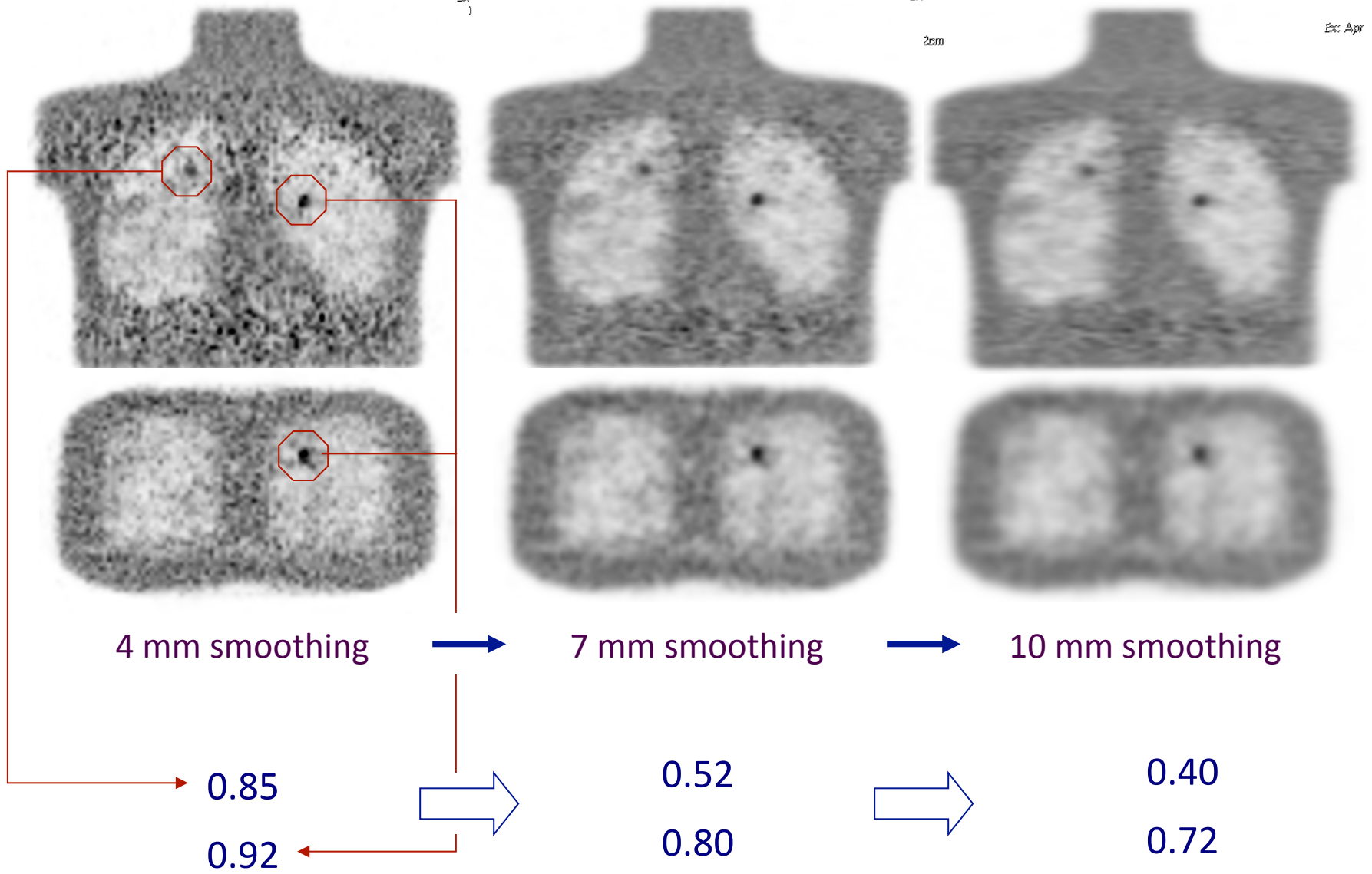
Modified NEMA NU-2 IQ Phantom

Recovery coefficient (RC) = measured/true (ideally 100%)



SNM Torso phantom with 1 cm spheres

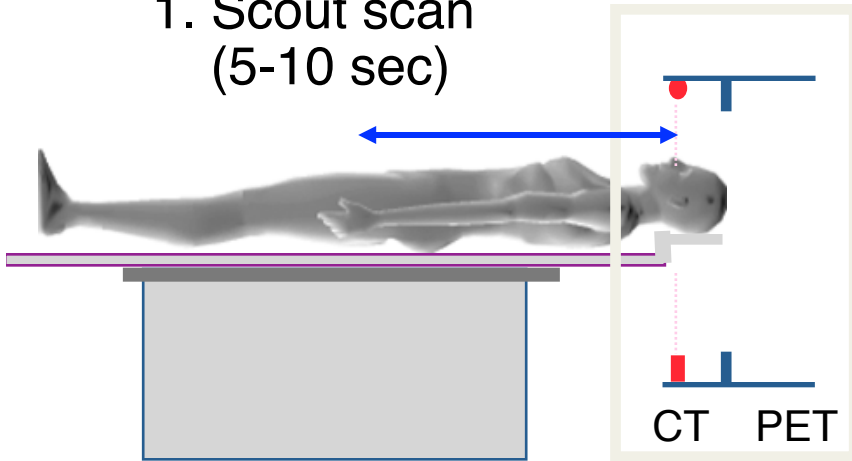
Increasing smoothing reduces both signal and noise



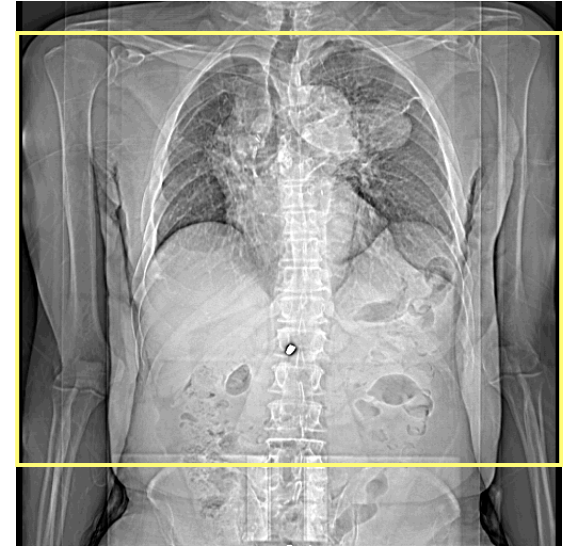
Clinical examples

Typical PET/CT Scan Protocol

1. Scout scan
(5-10 sec)

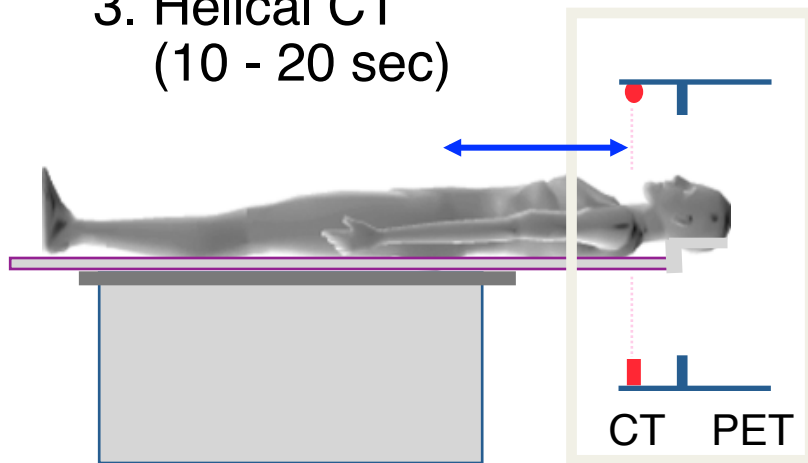


2. Selection
of scan
region



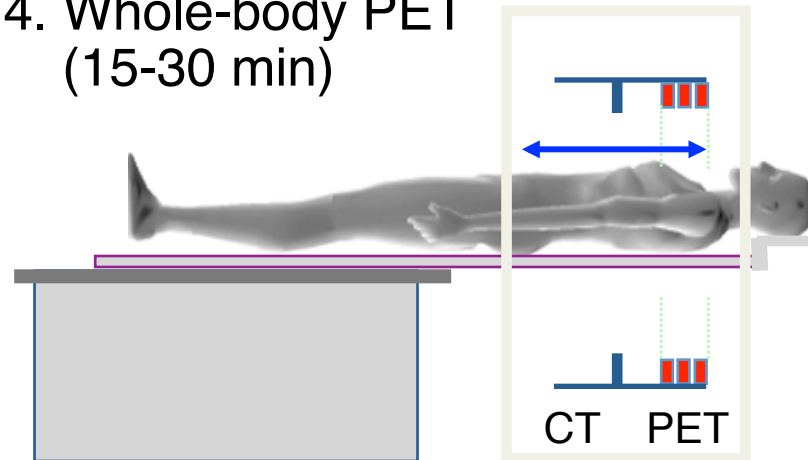
Scout scan image

3. Helical CT
(10 - 20 sec)



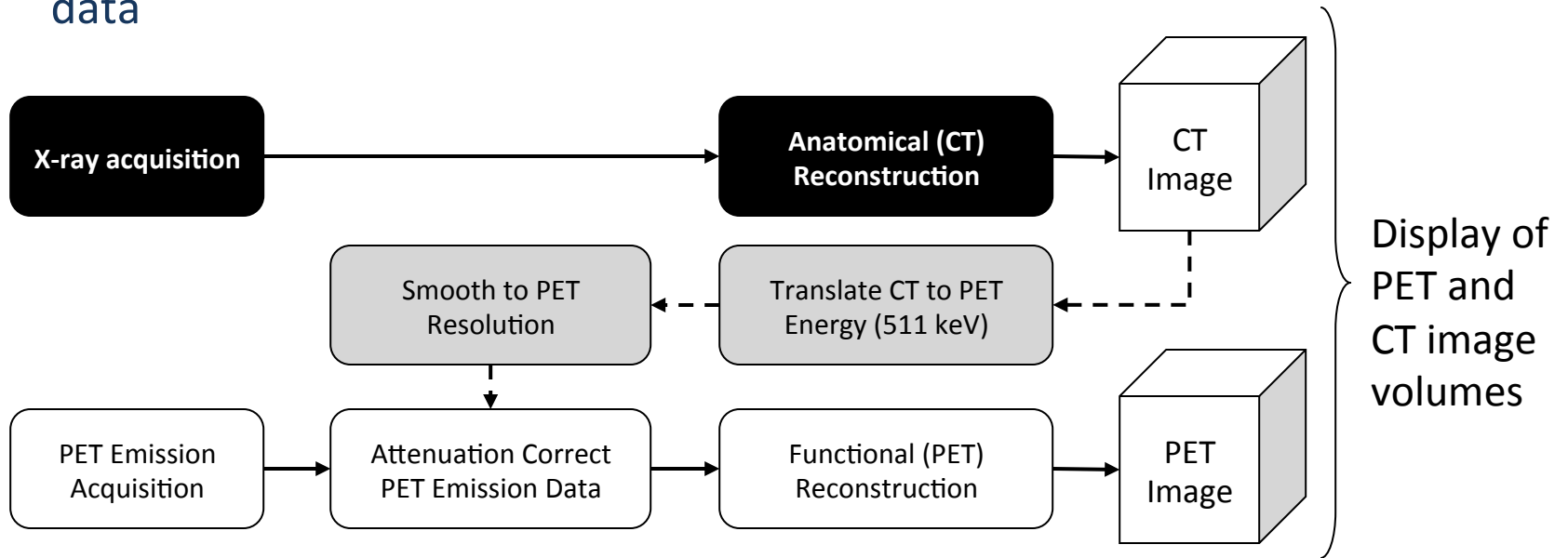
Paul Kinahan

4. Whole-body PET
(15-30 min)



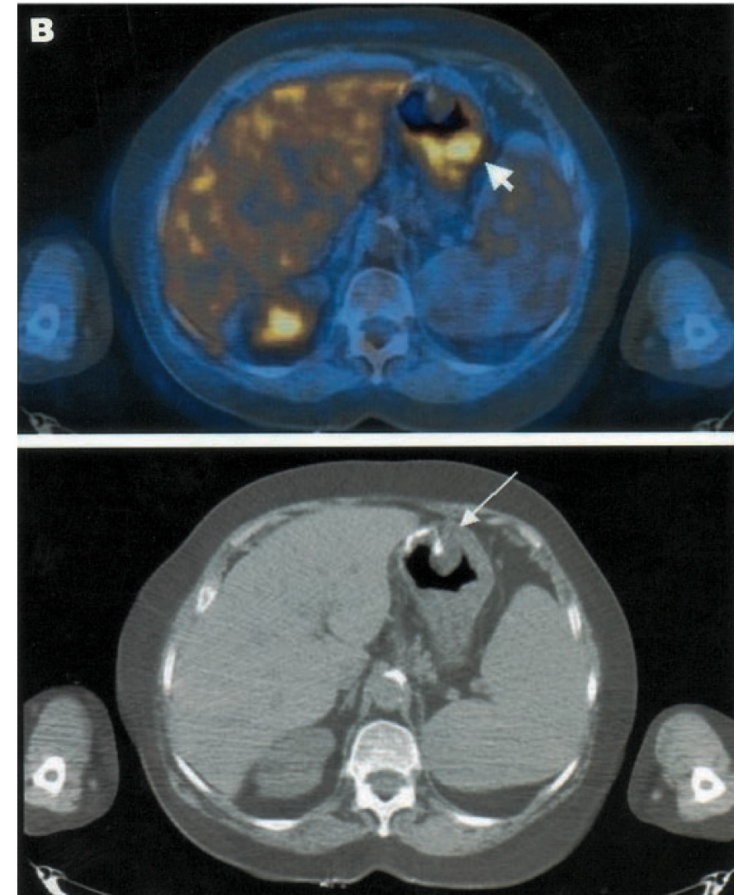
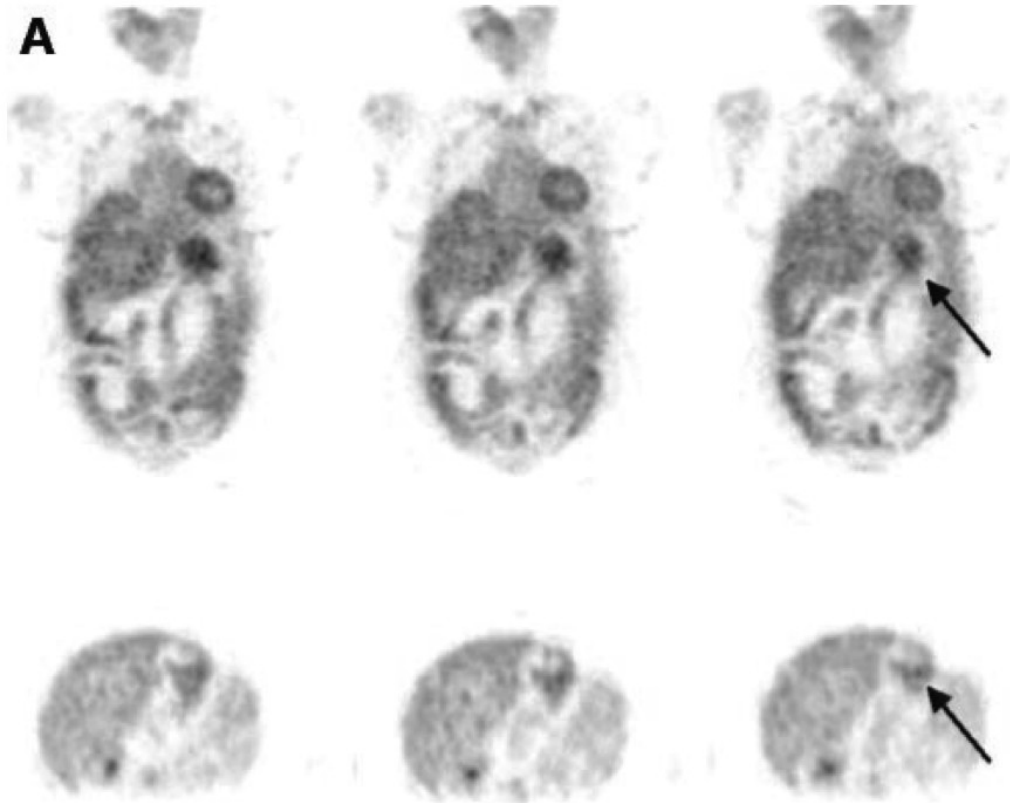
Reminder: Data Flow and Processing

- CT images are also used for calibration (attenuation correction) of the PET data



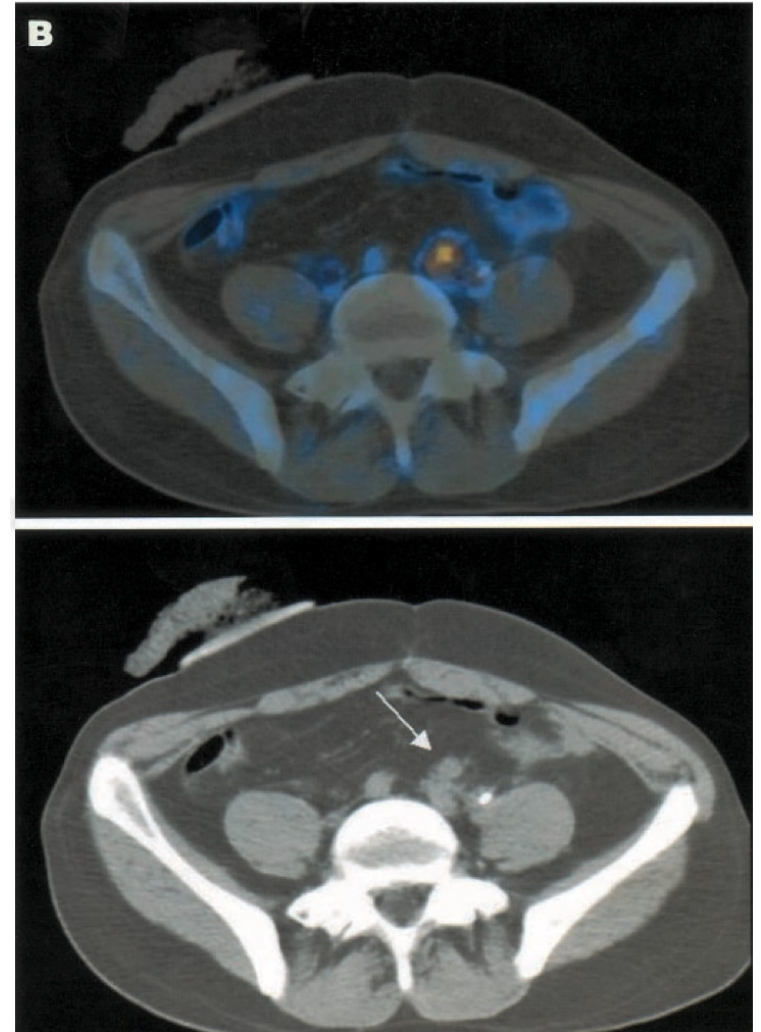
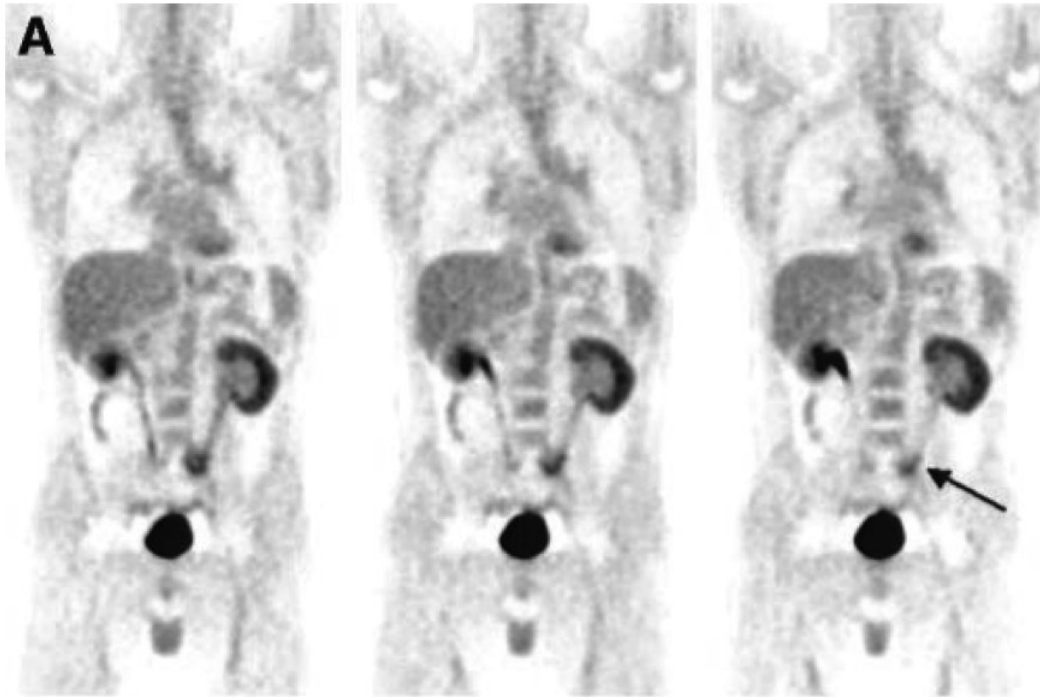
- Note that images are not really fused, but are displayed as fused or side-by-side with linked cursors

PET/CT for precise localization



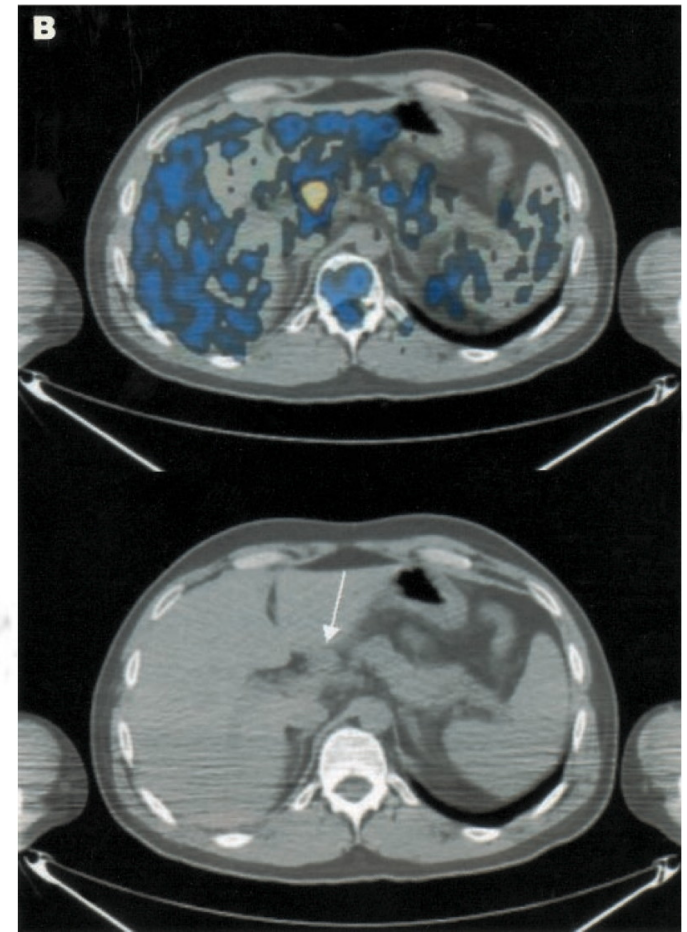
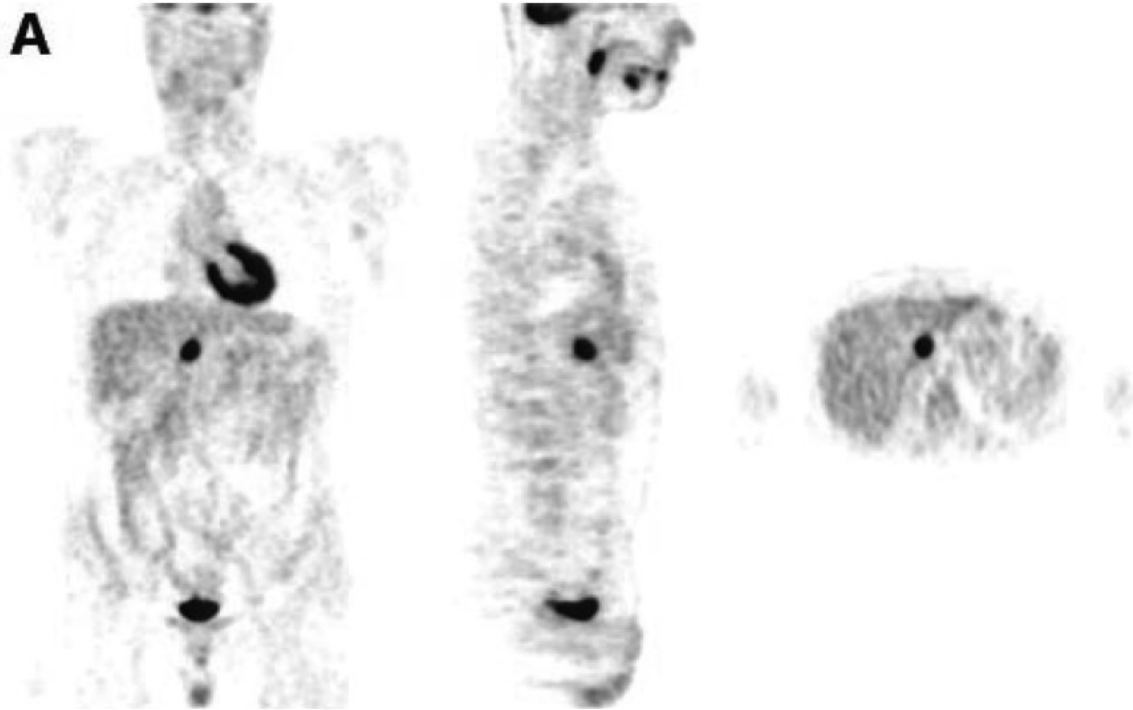
- 68-y-old man, 3 y after partial gastrectomy for adenocarcinoma of stomach
- Referred for 18F-FDG PET/CT for evaluation of mass detected on routine follow-up gastroscopy and equivocal biopsy results
- (A) 18F-FDG PET show increased 18F-FDG uptake in region of stomach (arrow)
- (B) Hybrid PET/CT axial image (top) precisely localizes and defines uptake as physiologic activity at gastric stump (arrowhead). Suspicious mass in anastomotic region (arrow), seen on corresponding hybrid and CT slices (bottom) obtained during same acquisition, shows no uptake of 18F-FDG.
- Findings on PET/CT were interpreted as physiologic 18F-FDG uptake in stomach and nonviable residual mass.
- Patient showed no evidence of disease for follow-up of 7 mo.

PET/CT for precise characterization



- A 35-y-old man, 22 mo after treatment for colon cancer
- Negative high-resolution contrast-enhanced CT and normal levels of serum tumor markers, was referred for 18F-FDG PET for further assessment of pelvic pain
- (A) Coronal PET images show area of increased 18F-FDG uptake in left pelvic region (arrow), interpreted as equivocal for malignancy, possibly related to inflammatory changes associated with ureteral stent or to physiologic bowel uptake
- (B) Hybrid PET/CT axial image (top) precisely localizes uptake to soft-tissue mass adjacent to left ureter, anterior to left iliac vessels. Mass (arrow) was detected only retrospectively on both diagnostic CT and CT component of hybrid imaging study
- Patient received chemotherapy, resulting in pain relief and decrease in size of pelvic mass on follow-up CT.

PET/CT for precise localization



- A 33-y-old man with Hodgkin's disease in left cervical region was referred for 18F-FDG PET for staging
- No other sites of disease were reported on CT
- (A) PET images show infradiaphragmatic focus of abnormal 18F-FDG uptake in medial border of liver, consistent with either liver involvement (stage IV disease?) or nodal disease in porta hepatis (stage III disease?)
- (B) Hybrid PET/CT axial image precisely localizes 18F-FDG uptake to adenopathy (abnormally large lymph node) at porta hepatis, only retrospectively detected on corresponding CT image (arrow)
- Patient was treated as having stage III disease and achieved complete response, showing no evidence of disease for follow-up of 12 mo.